Research Article

A Novel Algorithm for Studying the Effects of Squeezing Flow of a Casson Fluid between Parallel Plates on Magnetic Field

Abdul-Sattar J. A. Al-Saif[1] and Abeer Majeed Jasim [1,2]

[1]*Department of Mathematics, College of Education for Pure Science, University of Basrah, Basrah, Iraq*
[2]*Department of Mathematics, College of Science, University of Basrah, Basrah, Iraq*

Correspondence should be addressed to Abeer Majeed Jasim; abeer.jassem@yahoo.com

In this paper, the magneto hydrodynamic (MHD) squeezing flow of a non-Newtonian, namely, Casson, fluid between parallel plates is studied. The suitable one of similarity transformation conversion laws is proposed to obtain the governing MHD flow nonlinear ordinary differential equation. The resulting equation has been solved by a novel algorithm. Comparisons between the results of the novel algorithm technique and other analytical techniques and one numerical Range-Kutta fourth-order algorithm are provided. The results are found to be in excellent agreement. Also, a novel convergence proof of the proposed algorithm based on properties of convergent series is introduced. Flow behavior under the changing involved physical parameters such as squeeze number, Casson fluid parameter, and magnetic number is discussed and explained in detail with help of tables and graphs.

1. Introduction

Squeezing flow between parallel walls occurs in many industrial and biological systems. The unsteady squeezing flow of a viscous fluid between parallel plates in motion normal to their own surfaces is a great interest in hydrodynamical machines. The pioneer work and the basic formulation of squeezing flows under lubrication were assumed by Stefan [1]. In past researches over few decades, Reynolds [2] analyzed the squeezing flow between elliptic plates while Archibald [3] suggested the same problem for rectangular plates. The Reynolds equation was studied for squeezing flows which were not sufficient for some cases as was demonstrated by Jackson [4] and Usha and Sridharan [5]. The study on the motion of electrically conducting fluid in the presence of a magnetic field is called magneto hydrodynamics (MHD). In engineering, the application of MHD can be seen in the electromagnetic pump. The pumping motion of this device is caused by the Lorentz force. This force is produced when mutually perpendicular magnetic fields, and electric currents are applied in the direction perpendicular to the axis of a pipe containing conducting fluid [6]. The laws of

conservations under the similarity transformation for the squeezing flow of an electrically conducting Casson fluid, which was suggested by Wang [7], have been used to extract a highly nonlinear ordinary differential equation governing the magneto hydrodynamic (MHD). Many researchers have conducted numerous research attempts for the purpose of understanding and analyzing squeezing flows [8–14]. Duwairi et al. [15] investigated the effects of squeezing on heat transfer of a viscous fluid between parallel plates. Mohyud-Din et al. [16] have studied heat and mass transfer analysis for the flow of a nanofluid between rotating parallel plates while Mohyud-Din and Khan [17] analyzed the nonlinear radiation effects on squeezing flow of a Casson fluid between parallel disks. Ahmed et al. [18] assumed MHD flow of an incompressible fluid through porous medium between dilating and squeezing permeable plates. Khan et al. [19] have explained MHD squeezing flow between two finite plates, and Hayat et al. [20] have demonstrated the effect of squeezing flow of second grade fluid between two parallel disks. Naveed et al. [21] studied effects on magnetic field in squeezing flow of a Casson fluid between parallel plates. The main scope of this paper is to implement novel algorithm to obtain

analytical-approximate solution which depends mainly on the coefficients of powers series. This is close to the numerical solution for the squeezing flow of a Casson fluid between parallel plates; although the resulting series of the novel algorithm which contains initial conditions are known, the others are unknown and their values can be found through the boundary conditions that are defined. These series also contain physical parameters which can be compensated by constants, and the geometrical effects of these parameters would be investigated depending on the resulting solutions. In this work, it can be clearly seen that a novel algorithm is successfully applied to solve the equations of an unsteady squeeze of flow between parallel plates as well as to find an analytical-approximate solution. In contrast, it was found that our results from algorithm completely agree with the results obtained from the numerical solution through the application of Range-Kutta fourth-order method [RK-4], the numerical solutions of Wang [7], and variation of parameter method (VPM) [21]. The organization of this paper is as follows: The governing equations are derived in Section 2. Details of derivation of the novel algorithm have been written as steps in Section 3. The performance of the novel algorithm for the squeezing flow is applied in Section 4. In Section 5 the convergence analysis is presented. Results and discussions are given in Section 6. Finally, the conclusions are indicated in Section 7.

2. Governing Equations

We consider an incompressible flow of a Casson fluid between two parallel plates separated by a distance $y = \pm l(1 - \alpha t)^{1/2} = \pm h(t)$, where l is the initial gap between the plates (at a time $t = 0$). Additionally $\alpha > 0$ corresponds to a squeezing motion of both plates until they touch each other at $t = 1/\alpha$, for $\alpha < 0$; the plates bear a receding motion and dilate as described in Figure 1.

Rheological equation for Casson fluid is defined [22] as

$$
\tau_{ij} = \begin{cases} 2\left[\mu_B + \left(\dfrac{p_y}{2\pi}\right)\right] e_{ij}, & \pi > \pi_c \\[2mm] 2\left[\mu_B + \left(\dfrac{p_y}{2\pi_c}\right)\right] e_{ij}, & \pi_c > \pi, \end{cases} \tag{1}
$$

where $\pi = e_{ij}e_{ij}$ and e_{ij} is the $(i,j)th$ component of the deformation rate, π is the product of the component of deformation rate with itself, π_c is the critical value of the said product, μ_B is the plastic dynamic viscosity of the non-Newtonian fluid, and p_y is the yield stress of slurry fluid. We are also applying the following assumptions on the flow model:

   (i) The effects of induced magnetic and electric field produced due to the flow of electrically conducting fluid are negligible.

   (ii) No external electric field is present.

Under aforementioned constraints the conservation equations for the flow are

$$
\frac{\partial u}{\partial x} + \frac{\partial v}{\partial y} = 0, \tag{2}
$$

$$
\begin{aligned}
\frac{\partial u}{\partial t} &+ u\frac{\partial u}{\partial x} + v\frac{\partial u}{\partial y} \\
&= -\frac{1}{\rho}\frac{\partial p}{\partial x} + \frac{\mu}{\rho}\left(1 + \frac{1}{\gamma}\right)\left(2\frac{\partial^2 u}{\partial x^2} + \frac{\partial^2 u}{\partial y^2} + \frac{\partial^2 v}{\partial y \partial x}\right) \\
&\quad - \frac{\sigma\beta^2}{\rho}u,
\end{aligned} \tag{3}
$$

$$
\begin{aligned}
\frac{\partial v}{\partial t} &+ u\frac{\partial v}{\partial x} + v\frac{\partial v}{\partial y} \\
&= -\frac{1}{\rho}\frac{\partial p}{\partial y} + \frac{\mu}{\rho}\left(1 + \frac{1}{\gamma}\right)\left(2\frac{\partial^2 v}{\partial x^2} + \frac{\partial^2 v}{\partial y^2} + \frac{\partial^2 u}{\partial y \partial x}\right),
\end{aligned} \tag{4}
$$

where u and v are the velocity components in x and y directions, respectively, p is the pressure, μ/ρ is the dynamic viscosity of the fluid (ratio of Kinematic viscosity and density), $\gamma = \mu_B\sqrt{2\pi_c}/p_y$ is the Casson fluid parameter, and β is the magnitude of imposed magnetic field. Supporting conditions for the problem are as follows:

$$
u = 0,
$$
$$
v = v_w = \frac{dh}{dt}
$$
$$
at \ y = h(t),
$$
$$
\frac{\partial u}{\partial y} = 0,
$$
$$
v = 0
$$
$$
at \ y = 0, \tag{5}
$$

and we can simplify the above system of equations by eliminating the pressure term equations (3)-(4) and using (2). After cross differentiation and introducing vorticity ω

$$
\omega = \frac{\partial v}{\partial x} - \frac{\partial u}{\partial y}, \tag{6}
$$

we get

$$
\begin{aligned}
\frac{\partial \omega}{\partial t} &+ u\frac{\partial \omega}{\partial x} + v\frac{\partial \omega}{\partial y} = \frac{\mu}{\rho}\left(1 + \frac{1}{\gamma}\right)\left(\frac{\partial^2 \omega}{\partial x^2} + \frac{\partial^2 \omega}{\partial y^2}\right) \\
&\quad - \frac{\sigma\beta^2}{\rho}\frac{\partial u}{\partial y}.
\end{aligned} \tag{7}
$$

Transform introduced by Wang [7] for a two dimensional flow is stated as

$$
u = \frac{\alpha x}{\left[2(1 - \alpha t)^{1/2}\right]} f'(\eta), \tag{8}
$$

$$
v = \frac{-\alpha l}{\left[2(1 - \alpha t)^{1/2}\right]} f(\eta), \tag{9}
$$
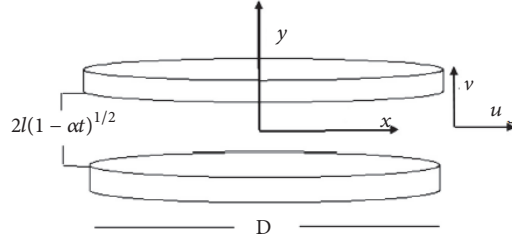
FIGURE 1: Schematic diagram for the flow problem.

where

$$\eta = \frac{y}{\left[l\left(1-\alpha\right)^{1/2}\right]}. \tag{10}$$

Substituting (8)-(10) in (7) and using (6) yield a nonlinear ordinary differential equation describing the Casson fluid flow as

$$\left(1+\frac{1}{\gamma}\right)f^{iv} - S\left(\eta f'''\left(\eta\right) + 3f'\left(\eta\right) + f'\left(\eta\right)f''\left(\eta\right)\right.$$
$$\left. - f\left(\eta\right)f'''\left(\eta\right)\right) - M^2 f''\left(\eta\right) = 0 \tag{11}$$

where $S = \alpha l^2 \rho/2\mu$ denotes the nondimensional Squeeze number and $M = l\beta\sqrt{\sigma(1-\alpha t)/\mu}$ is magnetic number. Boundary conditions for the problem by using (8)-(10) reduce to

$$f\left(0\right) = 0,$$
$$f''\left(0\right) = 0,$$
$$f\left(1\right) = 1, \tag{12}$$
$$f'\left(1\right) = 0,$$

and squeezing number S describes the movement of the plates ($S > 0$ corresponds to the plates moving apart, while $S < 0$ corresponds to collapsing movement of the plates). It is pertinent to mention here that for $M = 0$ and $\gamma \longrightarrow \infty$ our study reduces to the one obtained by Wang [7]. Skin friction coefficient is defined as

$$\frac{l^2}{x^2\left(1-\alpha t\right)}Re_x C_f = \left(1+\frac{1}{\gamma}\right)f''\left(1\right). \tag{13}$$

where

$$C_f = \frac{\mu}{\rho}\frac{\left(\partial u/\partial t\right)_{y=h(t)}}{v_w^2}, \tag{14}$$

$$Re_x = \frac{2lv_w^2}{vx\left(1-\alpha t\right)^{1/2}}, \tag{15}$$

3. The Basic Steps of the Novel Algorithm

This section describes how to obtain a novel algorithm to calculate the coefficients of the power series solution resulting from solving nonlinear ordinary differential equations

resulting from using transforms ((8)-(10)) to find analytical-approximate solution. These coefficients are important bases to construct the solution formula; therefore they can be computed recursively by differentiation ways. To illustrate the computation of these coefficients and derivation of the novel algorithm, we summarized the detailed new outlook in the following steps.

Step 1. Consider the nonlinear differential equation as follows:

$$H\left(f\left(\eta\right), f'\left(\eta\right), f''\left(\eta\right), f'''\left(\eta\right), \ldots, f^{(n-1)}\left(\eta\right), f^{(n)}\left(\eta\right)\right)$$
$$= 0, \tag{16}$$

and integrating (16) with respect to η on $[0, \eta]$ yields

$$f\left(\eta\right) = f\left(0\right) + f'\left(0\right)\eta + f''\left(0\right)\frac{\eta^2}{2!}, \ldots$$
$$+ f^{(n-1)}\left(0\right)\frac{\eta^{n-1}}{(n-1)!} + L^{-1}G\left[f\left(\eta\right)\right], \tag{17}$$

where

$$G\left[f\left(\eta\right)\right]$$
$$= H\left(f\left(\eta\right), f'\left(\eta\right), f''\left(\eta\right), \ldots, f^{(n-1)}\left(\eta\right)\right), \tag{18}$$
$$L^{-1} = \int_0^\eta \int_0^\eta \cdots \int_0^\eta \left(d\eta\right)^n.$$

Step 2. Assume that

$$G\left[f\left(\eta\right)\right] = \sum_{n=1}^{\infty}\frac{d^{n-1}G\left(f_0\left(\eta\right)\right)}{d\eta^{n-1}}, \tag{19}$$

rewriting (19)

$$G\left[f\left(\eta\right)\right] = G\left[f_0\left(\eta\right)\right] + G'\left[f_0\left(\eta\right)\right] + G''\left[f_0\left(\eta\right)\right]$$
$$+ G'''\left[f_0\left(\eta\right)\right] + G''''\left[f_0\left(\eta\right)\right] + \cdots, \tag{20}$$

and substituting (20) in (17), we obtain

$$f\left(\eta\right) = f_0 + f_1 + f_2 + f_3 + f_4 + \cdots, \tag{21}$$

where

$$f_0 = f(0) + f'(0)\eta + f''(0)\frac{\eta^2}{2!}\cdots$$

$$+ f^{(n-1)}(0)\frac{\eta^{(n-1)}}{(n-1)!},$$

$$f_1 = L^{-1}G[f_0(\eta)],$$

$$f_2 = L^{-1}G'[f_0(\eta)],$$

$$f_3 = L^{-1}G''[f_0(\eta)],$$

$$f_4 = L^{-1}G'''[f_0(\eta)],\ldots$$

(22)

Step 3. We focus on computing the derivatives of G with respect to η which is the crucial part of the proposed method. Let us start calculating $G[f(\eta)], G'[f(\eta)], G''[f(\eta)], G'''[f(\eta)],\ldots$

$$G[f(\eta)] = H\left(f(\eta), f'(\eta), f''(\eta), f'''(\eta), f''''(\eta),\right.$$
$$\left.\ldots, f^{(n-1)}(\eta)\right),$$

(23)

$$G'[f(\eta)] = \frac{dG[f(\eta)]}{d\eta} = G_f \cdot f_\eta + G_{f'} \cdot (f_\eta)' + \cdots$$
$$+ G_{f^{(n-1)}} \cdot (f_\eta)^{(n-1)},$$

(24)

$$G''[f(\eta)] = \frac{d^2G[f(\eta)]}{d\eta^2} = G_{ff} \cdot (f_\eta)^2 + G_{ff'} \cdot (f_\eta)'$$

$$\cdot f_\eta + G_{ff''} \cdot f_\eta (f_\eta)'' + \cdots + G_{ff^{(n-1)}} \cdot (f_\eta)(f_\eta)^{(n-1)}$$

$$+ G_f \cdot f_{\eta\eta} + G_{f'f} \cdot (f_\eta)' \cdot f_\eta + G_{f'f'} \cdot (f_\eta)'^2 + \cdots$$

$$+ G_{f'f^{(n-1)}} \cdot (f_\eta)'(f_\eta)^{(n-1)} + G_{f'} \cdot (f_{\eta\eta})' + G_{f''f} \cdot$$

$$(f_\eta)'' \cdot f_\eta + G_{f''f'} \cdot (f_\eta)'(f_\eta)'' + G_{f''f''} \cdot (f_\eta)''^2$$

$$+ G_{f''f^{(n-1)}} \cdot (f_\eta)''(f_\eta)^{(n-1)} + Gf'' \cdot (f_{\eta\eta})'' + \cdots$$

$$+ G_{f^{(n-1)}f} \cdot (f_\eta)^{(n-1)} \cdot f_\eta + G_{f^{(n-1)}f'} \cdot (f_\eta)^{(n-1)} \cdot (f_\eta)'$$

$$+ \cdots + G_{f^{(n-1)}f^{(n-1)}} \cdot (f_\eta)^{(n-1)2} + G_{f^{(n-1)}} \cdot (f_{\eta\eta})^{(n-1)},$$

(25)

$$G'''[f(\eta)] = \frac{d^3G[f(\eta)]}{d\eta^3} = G_{fff} \cdot (f_\eta)^3 + G_{fff'} \cdot$$

$$(f_\eta)^2 (f_\eta)' + \cdots + G_{fff^{(n-1)}} \cdot (f_\eta)^2 \cdot (f_\eta)^{(n-1)} + G_{ff} \cdot$$

$$2(f_\eta) \cdot f_{\eta\eta} + G_{ff'f} \cdot (f_\eta)'(f_\eta)^2 + G_{ff'f'} \cdot (f_\eta)'^2$$

$$\cdot (f_\eta) + \cdots + G_{ff'f^{(n-1)}} \cdot (f_\eta)'(f_\eta) \cdot (f_\eta)^{(n-1)}$$

$$+ G_{ff'} \cdot \left[(f_{\eta\eta})' \cdot f_\eta + (f_\eta)' \cdot f_{\eta\eta}\right] + G_{ff''f} \cdot (f_\eta)''$$

$$\cdot (f_\eta)^2 + G_{ff''f'} \cdot (f_\eta)''(f_\eta) \cdot (f_\eta)' + \cdots$$

$$+ G_{ff''f^{(n-1)}} \cdot (f_\eta)''(f_\eta) \cdot (f_\eta)^{(n-1)} + G_{ff''} \cdot \left[f_{\eta\eta}\cdot\right.$$

$$\left.(f_\eta)'' + f_\eta \cdot (f_{\eta\eta})''\right] + \cdots + G_{ff^{(n-1)}f} \cdot (f_\eta)^2 \cdot$$

$$(f_\eta)^{(n-1)} + G_{ff^{(n-1)}f'} \cdot (f_\eta) \cdot (f_\eta)' \cdot (f_\eta)^{(n-1)} + \cdots$$

$$+ G_{ff^{(n-1)}f^{(n-1)}} \cdot (f_\eta) \cdot (f_\eta)^{(n-1)2} + G_{ff^{(n-1)}} \cdot \left[(f_{\eta\eta})\cdot\right.$$

$$\left.(f_\eta)^{(n-1)} + (f_\eta)(f_{\eta\eta})^{(n-1)}\right] + G_{ff} \cdot f_{\eta\eta} \cdot (f_\eta)$$

$$+ G_{ff'} \cdot f_{\eta\eta} \cdot (f_\eta)' + \cdots + G_{ff^{(n-1)}} \cdot f_{\eta\eta} \cdot (f_\eta)^{(n-1)}$$

$$+ G_\eta \cdot f_{\eta\eta\eta} + G_{f'ff} \cdot (f_\eta)' (f_\eta)^2 + G_{f'f'f} \cdot (f_\eta)'^2$$

$$\cdot (f_\eta) + \cdots + G_{f'ff^{(n-1)}} \cdot (f_\eta)'(f_\eta) \cdot (f_\eta)^{(n-1)}$$

$$+ G_{f'f} \cdot \left[(f_{\eta\eta})' \cdot f_\eta + (f_\eta)' \cdot f_{\eta\eta}\right] + G_{f'f'f} \cdot (f_\eta)'^2 \cdot$$

$$f_z + G_{f'f'f'} \cdot (f_\eta)'^3 + \cdots + G_{f'f'f^{(n-1)}} \cdot (f_\eta)'^2 \cdot$$

$$(f_\eta)^{(n-1)} + G_{f'f'} \cdot 2(f_\eta)' \cdot (f_{\eta\eta})' + \cdots$$

$$+ G_{f^{(n-1)}f^{(n-1)}f} \cdot (f_\eta)^{(n-1)2} \cdot f_\eta + G_{f^{(n-1)}f^{(n-1)}f'} \cdot$$

$$(f_\eta)^{(n-1)2} \cdot (f_\eta)' + \cdots + G_{f^{(n-1)}f^{(n-1)}f^{(n-1)}} \cdot (f_\eta)^{(n-1)3}$$

$$+ G_{f^{(n-1)}f^{(n-1)}} \cdot 2 \cdot (f_\eta)^{(n-1)} \cdot (f_{\eta\eta})^{(n-1)} + G_{f^{(n-1)}f} \cdot$$

$$(f_{\eta\eta})^{(n-1)} \cdot f_\eta + G_{f^{(n-1)}f'} \cdot (f_{\eta\eta})^{(n-1)} \cdot (f_\eta)' + \cdots$$

$$+ G_{f^{(n-1)}f^{(n-1)}} \cdot (f_{\eta\eta})^{(n-1)} \cdot (f_\eta)^{(n-1)} + G_{f^{(n-1)}} \cdot$$

$$(f_{\eta\eta\eta})^{(n-1)}.$$

$$\vdots$$

(26)

We see that the calculations become more complicated in the second and third derivatives because of the numerous calculations. Consequently, the systematic structure on calculation is extremely important. Fortunately, due to the assumption that the operator G and the solution f are analytic functions, the mixed derivatives are equivalent.

We note that the derivatives function to f is unknown, so we suggest the following hypothesis

$$f_\eta = f_1 = L^{-1}G[f_0(\eta)],$$

$$f_{\eta\eta} = f_2 = L^{-1}G'[f_0(\eta)],$$

$$f_{\eta\eta\eta} = f_3 = L^{-1}G''\left[f_0\left(\eta\right)\right],$$

$$f_{\eta\eta\eta\eta} = f_4 = L^{-1}G'''\left[f_0\left(\eta\right)\right],$$

$$f_{\eta\eta\eta\eta\eta} = f_5 = L^{-1}G''''\left[f_0\left(\eta\right)\right],\ldots$$

$$(27)$$

Therefore (23)-(26) are evaluated by

$$G\left[f_0\left(\eta\right)\right]$$

$$(28)$$

$$= H\left(f_0\left(\eta\right), f_0'\left(\eta\right), f_0''\left(\eta\right), \ldots, f_0^{(n-1)}\left(\eta\right)\right),$$

$$G'\left[f_0\left(\eta\right)\right] = G_{f_0}.f_1 + G_{f_0'}.\left(f_1\right)' + G_{f_0''}.\left(f_1\right)'' + \cdots$$

$$(29)$$

$$+ G_{f_0^{(n-1)}}.\left(f_1\right)^{(n-1)},$$

$$G''\left[f_0\left(\eta\right)\right] = G_{f_0 f_0}.\left(f_1\right)^2 + G_{f_0 f_0'}.\left(f_1\right)' f_1$$

$$+ G_{f_0 f_0''}.f_1\left(f_1\right)'' + \cdots + G_{f_0 f_0^{(n-1)}}.\left(f_1\right)\left(f_1\right)^{(n-1)}$$

$$+ G_{f_0}.f_2 + G_{f_0' f_0}.\left(f_1\right)'.f\left(_1\right) + G_{f_0' f_0'}.\left(f_1\right)'^2 + \cdots$$

$$+ G_{f_0' f_0^{(n-1)}}.\left(f_1\right)'\left(f_1\right)^{(n-1)} + G_{f_0'}.\left(f_2\right)'$$

$$+ G_{f_0'' f_0}.\left(f_1\right)''.f_1 + G_{f_0'' f_0'}.\left(f_1\right)'\left(f_1\right)''$$

$$+ G_{f_0'' f_0''}.\left(f_1\right)''^2 + \cdots + G_{f_0'' f_0^{(n-1)}}.\left(f_1\right)''\left(f_1\right)^{(n-1)}$$

$$+ G_{f_0''}.\left(f_2\right)'' + G_{f^{(n-1)} f}.\left(f_1\right)^{(n-1)}.f_1$$

$$+ G_{f_0^{(n-1)} f_0'}.\left(f_1\right)^{(n-1)}.\left(f_1\right)' + \cdots$$

$$+ G_{f_0^{(n-1)} f_0^{(n-1)}}.\left(f_1\right)^{(n-1)2} + \cdots + G_{f_0^{(n-1)}}.\left(f_2\right)^{(n-1)},$$

$$(30)$$

$$G'''\left[f_0\left(\eta\right)\right] = G_{f_0 f_0 f_0}.\left(f_1\right)^3 + G_{f_0 f_0 f_0'}.\left(f_1\right)^2\left(f_1\right)'$$

$$+ \cdots + G_{f_0 f_0 f_0^{(n-1)}}.\left(f_1\right)^2.\left(f_1\right)^{(n-1)}$$

$$+ G_{f_0 f_0}.2\left(f_1\right).f_2 + G_{f_0 f_0' f_0}.\left(f_1\right)'\left(f_1\right)^2$$

$$+ G_{f_0 f_0' f_0'}.\left(f_1\right)'^2\left(f_1\right) + \cdots$$

$$+ G_{f_0 f_0' f_0^{(n-1)}}.\left(f_1\right)'\left(f_1\right).\left(f_1\right)^{(n-1)}$$

$$+ G_{f_0 f_0'}.\left[\left(f_2\right)'.f_z + \left(f_1\right)'.f_2\right]$$

$$+ G_{f_0 f_0'' f_0}.\left(f_1\right)''\left(f_1\right)^2 + G_{f_0 f_0'' f_0'}.\left(f_1\right)''\left(f_1\right).\left(f_1\right)'$$

$$+ \cdots + G_{f_0 f_0'' f_0^{(n-1)}}.\left(f_1\right)''\left(f_1\right).\left(f_1\right)^{(n-1)}$$

$$+ G_{f_0 f_0'''}.\left[f_2.\left(f_1\right)'' + f_1.\left(f_2\right)''\right] + \cdots$$

$$+ G_{f_0 f_0^{(n-1)} f_0}.\left(f_1\right)^2.\left(f_1\right)^{(n-1)}$$

$$+ G_{f_0 f_0^{(n-1)} f_0'}.\left(f_1\right).\left(f_1\right)'.\left(f_1\right)^{(n-1)} + \cdots$$

$$+ G_{f_0 f_0^{(n-1)} f_0^{(n-1)}}.\left(f_1\right).\left(f_1\right)^{2(n-1)}$$

$$+ G_{f_0 f_0^{(n-1)}}.\left[\left(f_2\right).\left(f_2\right)^{(n-1)} + \left(f_1\right)\left(f_2\right)^{(n-1)}\right]$$

$$+ G_{f_0 f_0}.f_2.\left(f_1\right) + G_{f_0 f_0'}.f_2.\left(f_1\right)' + \cdots$$

$$+ G_{f_0 f_0^{(n-1)}}.f_2.\left(f_1\right)^{(n-1)} + G_{f_0}.f_3$$

$$+ G_{f_0' f_0 f_0}.\left(f_1\right)'\left(f_1\right)^2 + G_{f_0' f_0' f_0}.\left(f_1\right)'^2\left(f_1\right) + \cdots$$

$$+ G_{f_0' f_0 f_0^{(n-1)}}.\left(f_1\right)'\left(f_1\right).\left(f_1\right)^{(n-1)}$$

$$+ G_{f_0' f_0}.\left[\left(f_2\right)'.f_1 + \left(f_1\right)'.f_1\right] + G_{f_0' f_0' f_0}.\left(f_1\right)'^2.f_1$$

$$+ G_{f_0' f_0' f_0'}.\left(f_1\right)'^3 + \cdots$$

$$+ G_{f_0' f_0' f_0^{(n-1)}}.\left(f_1\right)'^2.\left(f_1\right)^{(n-1)}$$

$$+ G_{f_0' f_0'}.2\left(f_1\right)'.\left(f_2\right)' + \cdots$$

$$+ G_{f_0^{(n-1)} f_0^{(n-1)} f_0}.\left(f_1\right)^{(n-1)2}.f_1$$

$$+ G_{f_0^{(n-1)} f_0^{(n-1)} f_0'}.\left(f_1\right)^{(n-1)2}.\left(f_1\right)' + \cdots$$

$$+ G_{f_0^{(n-1)} f_0^{(n-1)} f_0^{(n-1)}}.\left(f_1\right)^{(n-1)3}$$

$$+ G_{f_0^{(n-1)} f_0^{(n-1)}}.2.\left(f_1\right)^{(n-1)}.\left(f_2\right)^{(n-1)}$$

$$+ G_{f_0^{(n-1)} f_0}.\left(f_2^{(n-1)}.f_1 + G_{f_0^{(n-1)} f_0'}.\left(f_2\right)^{(n-1)}.\left(f_1\right)'\right.$$

$$+ \cdots + G_{f_0^{(n-1)} f_0^{(n-1)}}.\left(f_2\right)^{(n-1)}.\left(f_1\right)^{(n-1)}$$

$$+ G_{f_0^{(n-1)}}.\left(f_3\right)^{(n-1)},$$

$$\vdots$$

$$(31)$$

Step 4. Substituting (28)-(31) in (21) we will get the required analytical-approximate solution for (16).

4. Application

The novel algorithm described in the previous section can be used as a powerful solver to the nonlinear differential

equations of squeezing flow between two parallel plates (11) - (12) in order to find a new analytical-approximate solution. From Step 1 we have

$$f(\eta) = f(0) + f'(0)\eta + f''(0)\frac{\eta^2}{2!} + f'''(0)\frac{\eta^3}{3!}$$

$$+ L^{-1}\left[\frac{\gamma S}{1+\gamma}\left(\eta f'''(\eta) + 3f'(\eta) + f'(\eta)f''(\eta)\right. \right. \quad (32)$$

$$\left. \left. - f(\eta)f'''(\eta)\right) + \frac{\gamma M^2}{1+\gamma}f''(\eta)\right],$$

and we rewrite (32) as follows

$$f(\eta) = A_1 + A_2\eta + A_3\frac{\eta^2}{2!} + A_4\frac{\eta^3}{3!} + L^{-1}G[f(\eta)], \quad (33)$$

where

$$A_1 = f(0),$$
$$A_2 = f'(0),$$
$$A_3 = f''(0),$$
$$A_4 = f'''(0),$$

$$G[f] = \frac{\gamma S}{1+\gamma}\left(\eta f'''(\eta) + 3f'(\eta) + f'(\eta)f''(\eta)\right. \quad (34)$$

$$\left. - f(\eta)f'''(\eta)\right) + \frac{\gamma M^2}{1+\gamma}f''(\eta),$$

$$\text{and } L^{-1}(.) = \int_0^\eta \int_0^\eta \int_0^\eta \int_0^\eta (d\eta)^4.$$

From the boundary conditions, (33) becomes

$$f(\eta) = A_2\eta + A_4\frac{\eta^3}{3!} + L^{-1}[G[f(\eta)]], \quad (35)$$

and from Step 2 we have

$$f_0 = A_2\eta + A_4\frac{\eta^3}{3!},$$
$$f_1 = L^{-1}G[f_0(\eta)],$$
$$f_2 = L^{-1}G'[f_0(\eta)], \quad (36)$$
$$f_3 = L^{-1}G''[f_0(\eta)],$$
$$f_4 = L^{-1}G'''[f_0(\eta)],\ldots$$

Step 3 yields

$$G[f(\eta)] = \frac{\gamma S}{1+\gamma}\left(\eta f'''(\eta) + 3f'(\eta)\right. \quad (37)$$

$$\left. + f'(\eta)f''(\eta) - f(\eta)f'''(\eta)\right) + \frac{\gamma M^2}{1+\gamma}f''(\eta)\Big],$$

$$G'[f(\eta)] = \frac{dG[f(\eta)]}{d\eta} = G_f\cdot f_\eta + G_{f'}\cdot(f_\eta)' + G_{f''}\cdot \quad (38)$$

$$(f_\eta)'' + G_{f'''}\cdot(f_\eta)''',$$

$$G''[f(\eta)] = \frac{d^2G[f(\eta)]}{d\eta^2} = G_{ff}\cdot(f_\eta)^2 + 2.G_{ff'}\cdot$$

$$f_\eta(f_\eta)' + 2.G_{ff''}\cdot f_\eta(f_\eta)'' + 2.G_{ff'''}\cdot f_\eta(f_\eta)'''$$

$$+ G_{f'f'}\cdot(f_\eta)'^2 + 2.G_{f'f''}\cdot(f_\eta)'(f_\eta)'' + 2.G_{f'f'''}\cdot \quad (39)$$

$$(f_\eta)'(f_\eta)''' + G_{f''f''}\cdot(f_\eta)''^2 + 2.G_{f''f'''}\cdot(f_\eta)''$$

$$\cdot(f_\eta)''' + G_{f'''f'''}\cdot(f_\eta)'''^2 + G_f\cdot f_{\eta\eta} + G_{f'}\cdot(f_{\eta\eta})'$$

$$+ G_{f''}\cdot(f_{\eta\eta})'' + G_{f'''}\cdot(f_{\eta\eta})''',$$

$$G'''[f(\eta)] = \frac{d^3G[f(\eta)]}{d\eta^3} = G_{fff}(f_\eta)^3 + 3.$$

$$G_{fff'}(f_\eta)^2\cdot(f_\eta)' + 3.G_{fff''}(f_\eta)^2\cdot(f_\eta)'' + 3.$$

$$G_{fff'''}(f_\eta)^2\cdot(f_\eta)''' + 3.G_{ff'f'}(f_\eta)(f_\eta)'^2 + 4.$$

$$G_{ff'f''}\cdot(f_\eta)\cdot(f_\eta)'\cdot(f_\eta)'' + 4.G_{ff'f'''}\cdot(f_\eta)\cdot(f_\eta)'\cdot$$

$$(f_\eta)''' + 3.G_{ff''f''}\cdot(f_\eta)(f_\eta)''^2 + 4.G_{ff''f'''}\cdot(f_\eta)\cdot$$

$$(f_\eta)''\cdot(f\eta)''' + 3.G_{ff'''f'''}\cdot(f_\eta)\cdot(f_\eta)'''^2 + G_{f'f'f'}\cdot$$

$$(f_\eta)'^3 + 3.G_{f'f'f''}\cdot(f_\eta)'^2\cdot(f_\eta)'' + G_{f'f'f'''}\cdot(f_\eta)'^2\cdot$$

$$(f_\eta)''' + 4.G_{f'f''f}\cdot(f_\eta)'\cdot f_\eta\cdot(f_\eta)'' + 3.G_{f'f''f''}\cdot$$

$$(f_\eta)'\cdot(f_\eta)''^2 + 4.G_{f'f''f'''}\cdot(f_\eta)'\cdot(f_\eta)''\cdot(f_\eta)'''$$

$$+ 4.G_{f'f'''f}\cdot(f_\eta)'\cdot f_\eta\cdot(f_\eta)''' + 4.G_{f'f'''f''}\cdot(f_\eta)'\cdot$$

$$(f_\eta)''\cdot(f_\eta)''' + 3.G_{f'f'''f'''}\cdot(f_\eta)'\cdot(f_\eta)'''^2$$

$$+ G_{f''f''f''}\cdot(f_\eta)''^3 + 3.G_{f''f''f'''}\cdot(f_\eta)''^2\cdot(f_\eta)'''$$

$$+ 3.G_{f''f'''f'''}\cdot(f_\eta)'''^2\cdot(f_\eta)'' + G_{f'''f'''f'''}\cdot(f_\eta)'''^3$$

$$+ 3.G_{ff}\cdot f_{\eta\eta}\cdot f_\eta + 3.G_{ff'}\cdot f_{\eta\eta}\cdot(f_\eta)' + 3.G_{ff''}\cdot f_{\eta\eta}\cdot$$

$$(f_\eta)'' + 3.G_{ff'''}\cdot f_{\eta\eta}\cdot(f_\eta)''' + G_f\cdot f_{\eta\eta\eta} + 3.G_{f'f}\cdot$$

$$(f_{\eta\eta})'(f_\eta) + 3.G_{f'f'}.(f_{\eta\eta})'(f_\eta)' + 3.G_{f'f''}.$$

$$(f_{\eta\eta})'(f_\eta)'' + 3.G_{f'f'''}.(f_{\eta\eta})'(f_\eta)'' + G_{f'}.$$

$$(f_{\eta\eta\eta})' + 3.G_{f''f}.(f_{\eta\eta})''.(f_\eta) + 3.G_{f''f'}.(f_{\eta\eta})''.$$

$$(f_\eta)' + 3.G_{f''f''}.(f_{\eta\eta})''.(f_\eta)'' + 3.G_{f''f'''}.(f_{\eta\eta})''.$$

$$(f_\eta)''' + G_{f''}.(f_{\eta\eta\eta})'' + 3.G_{f'''f}.(f_{\eta\eta})'''.(f_\eta)$$

$$+ 3.G_{f'''f'}.(f_{\eta\eta})'''.(f_\eta)' + 3.G_{f'''f''}.(f_{\eta\eta})'''.(f_\eta)''$$

$$+ 3.G_{f'''f'''}.(f_{\eta\eta})'''.(f_\eta)''' + G_{f'''}.(f_{\eta\eta\eta})''',$$

$$\vdots \tag{40}$$

We note that the derivatives of f with respect to η that are given in (27) can be computed by (37)-(40) as

$$G[f_0(\eta)] = \frac{\gamma S}{1+\gamma}\left((\eta.f_0'''(\eta) + 3.f_0'(\eta)\right. \\ \left. + f_0'(\eta).f_0''(\eta) - f_0(\eta).f_0'''(\eta)) + M^2 f_0''(\eta)\right), \tag{41}$$

$$G'[f_0(\eta)] = G_{f_0}.f_1 + G_{f_{0'}}.(f_1)' + G_{f_0''}.(f_1)'' \\ + G_{f_0'''}.(f_1)''', \tag{42}$$

$$G''[f_0(\eta)] = G_{f_0 f_0}.(f_1)^2 + 2.G_{f_0 f_0'}.f_1(f_1)' + 2.$$
$$G_{f_0 f_0''}.f_1(f_1)'' + 2.G_{f_0 f_0'''}.f_1(f_1)''' + G_{f_0' f_0'}.(f_1)'^2$$
$$+ 2.G_{f_0' f_0''}.(f_1)'(f_1)'' + 2.G_{f_0' f_0'''}.(f_1)'(f_1)'''$$
$$+ G_{f_0'' f_0''}.(f_1)''^2 + 2.G_{f_0'' f_0'''}.(f_1)''(f_1)'''$$
$$+ G_{f_0''' f_0'''}.(f_1)'''^2 + G_{f_0}.f_2 + G_{f_0'}.(f_2)' + G_{f_0''}.$$
$$(f_2)'' + G_{f_0'''}.(f_2)''', \tag{43}$$

$$G'''[f_0(\eta)] = G_{f_0 f_0 f_0}(f_1)^3 + 3.G_{f_0 f_0 f_0'}(f_1)^2.(f_1)'$$
$$+ 3.G_{f_0 f_0 f_0''}(f_1)^2.(f_1)'' + 3.G_{f_0 f_0 f_0'''}(f_1)^2.(f_1)'''$$
$$+ 3.G_{f_0 f_0' f_0'}.(f_1)(f_1)'^2 + 4.G_{f_0 f_0' f_0''}.(f_1).(f_1)'.$$
$$(f_1)'' + 4.G_{f_0 f_0' f_0'''}.(f_1).(f_1)'.(f_1)''' + 3.G_{f_0 f_0'' f_0''}.$$
$$(f_1)(f_1)''^2 + 4.G_{f_0 f_0'' f_0'''}.(f_1).(f_1)''.(f1)''' + 3.$$
$$G_{f_0 f_0''' f_0'''}.(f_1).(f_1)'''^2 + G_{f_0' f_0' f_0'}.(f_1)'^3 + 3.$$
$$G_{f_0' f_0' f_0''}.(f_1)'^2.(f_1)'' + G_{f_0' f_0' f_0'''}.(f_1)'^2.(f_1)''' + 4.$$
$$G_{f_0' f_0'' f_0}.(f_1)'.f_1.(f_1)'' + 3.G_{f_0' f_0'' f_0''}.(f_1)'.(f_1)''^2$$

$$+ 4.G_{f_0' f_0'' f_0'''}.(f_1)'.(f_1)''.(f_1)''' + 4.G_{f_0' f_0''' f_0}.(f_1)'.$$
$$f_1.(f_1)''' + 4.G_{f_0' f_0''' f_0'''}.(f_1)'.(f_1)''.(f_1)''' + 3.$$
$$G_{f_0' f_0''' f_0'''}.(f_1)'.(f_1)''^2 + G_{f_0'' f_0'' f_0''}.(f_1)''^3 + 3.$$
$$G_{f_0'' f_0'' f_0'''}.(f_1)''^2.(f_1)''' + 3.G_{f_0'' f_0''' f_0'''}.(f_1)''^2.(f_1)''$$
$$+ G_{f_0''' f_0''' f_0'''}.(f_1)'''^3 + 3.G_{f_0 f_0}.f_2.f_1 + 3.G_{f_0 f_0'}.f_2.$$
$$(f_1)' + 3.G_{f_0 f_0''}.f_2.(f_1)'' + 3.G_{f_0 f_0'''}.f_2.(f_1)'''$$
$$+ G_{f_0}.f_3 + 3.G_{f_0' f_0}.(f_2)'(f_1) + 3.G_{f_0' f_0'}.(f_2)'(f_1)'$$
$$+ 3.G_{f_0' f_0''}.(f_2)'(f_1)'' + 3.G_{f_0' f_0'''}.(f_2)'(f_1)''$$
$$+ G_{f_0'}.(f_3)' + 3.G_{f_0'' f_0}.(f_2)''.(f_1) + 3.G_{f_0'' f_0'}.$$
$$(f_2)''.(f_1)' + 3.G_{f_0'' f_0''}.(f_2)''.(f_1)'' + 3.G_{f_0'' f_0'''}.$$
$$(f_2)''.(f_1)''' + G_{f_0''}.(f_3)'' + 3.G_{f_0''' f_0}.(f_2)'''.(f_1)$$
$$+ 3.G_{f_0''' f_0'}.(f_2)'''.(f_1)' + 3.G_{f_0''' f_0''}.(f_2)'''.(f_1)''$$
$$+ 3.G_{f_0''' f_0'''}.(f_2)'''.(f_1)''' + G_{f_0'''}.(f_3)''',$$

$$\vdots \tag{44}$$

Now, we need to extract the first derivatives of G as follows:

$$G_{f_0} = -\frac{\gamma S}{1+\gamma}f_0'''(\eta),$$

$$G_{f_0 f_0} = G_{f_0 f_0'} = G_{f_0 f_0''} = 0,$$

$$G_{f_0 f_0'''} = -\frac{\gamma S}{1+\gamma},$$

$$G_{f_0 f_0 f_0} = G_{f_0 f_0' f_0} = G_{f_0 f_0' f_0'} = G_{f_0 f_0'' f_0'} = G_{f_0 f_0 f_0'}$$
$$= G_{f_0 f_0''' f_0'''} = G_{f_0 f_0'' f_0''} = 0,$$

$$G_{f_0'} = \frac{\gamma S}{1+\gamma} = (3 + f_0''(\eta)),$$

$$G_{f_0' f_0} = G_{f_0' f_0'} = G_{f_0' f_0'''} = 0,$$

$$G_{f_0' f_0''} = \frac{\gamma S}{1+\gamma},$$

$$G_{f_0' f_0 f_0} = G_{f_0' f_0' f_0} = G_{f_0' f_0' f_0'} = G_{f_0' f_0'' f_0'} = G_{f_0' f_0''' f_0'}$$
$$= G_{f_0' f_0''' f_0'''} = G_{f_0' f_0'' f_0''} = 0,$$

$$G_{f_0''} = \frac{\gamma S}{1+\gamma}f'(\eta) + \frac{\gamma M^2}{1+\gamma},$$

$$G_{f_0'' f_0} = G_{f_0'' f_0''} = G_{f_0'' f_0'''} = 0,$$

$$G_{f_0'' f_0'} = \frac{\gamma S}{1 + \gamma},$$

$$G_{f_0'' f_0 f_0} = G_{f_0'' f_0' f_0} = G_{f_0'' f_0' f_0'} = G_{f_0'' f_0'' f_0'} = G_{f_0'' f_0'' f_0'}$$

$$= G_{f_0'' f_0''' f_0'''} = G_{f_0'' f_0''' f_0'''} = 0,$$

$$G_{f_0'''} = \frac{\gamma S \eta}{1 + \gamma} - \frac{\gamma S}{1 + \gamma} f_0(\eta),$$

$$G_{f_0''' f_0'} = G_{f_0''' f_0''} = G_{f_0''' f_0'''} = 0,$$

$$G_{f_0''' f_0} = -\frac{\gamma S}{1 + \gamma},$$

$$G_{f_0''' f_0 f_0} = G_{f_0''' f_0' f_0} = G_{f_0''' f_0' f_0'} = G_{f_0''' f_0'' f_0'} = G_{f_0''' f_0''' f_0'}$$

$$= G_{f_0''' f_0''' f_0'''} = 0,$$

$$(45)$$

and from (36) by using (41)-(45), we obtain

$$f_0 = A_2 \eta + \frac{1}{6} A_4 \eta^3, \tag{46}$$

$$f_1 = \frac{1}{2520} r S A_4^2 \eta^7 + \frac{1}{120} r \left(4 S A_4 + M^2 A_4\right) \eta^5, \tag{47}$$

$$f_2 = \left(\frac{1}{210} r^2 S^2 A_4 + \frac{1}{504} r^2 S M^2 A_4 - \frac{1}{630} r^2 A_2 S^2 A_4\right.$$

$$\left. - \frac{1}{2520} r^2 S A_2 M^2 A_4 + \frac{1}{5040} r^2 M^4 A_4\right) \eta^7$$

$$- \left(\frac{1}{45360} r^2 S^2 A_4^2 A_2 - \frac{1}{60480} r^2 M^2 S A_4^2\right.$$

$$\left. - \frac{1}{11340} r^2 S^2 A_4^2\right) \eta^9 - \frac{1}{2494800} r^2 S^2 A_4^3 \eta^{11}, \tag{48}$$

$$f_3 = \left(\frac{1}{1890} r^3 S^3 A_4 + \frac{13}{45360} r^3 S^2 A_4 M^2\right.$$

$$+ \frac{-1}{2268} r^3 A_2 S^3 A_4 + \frac{-1}{5670} r^3 S^2 A_2 M^2 A_4$$

$$+ \frac{1}{20160} r^3 S M^4 A_4 + \frac{1}{11340} r^3 A_2^2 S^3 A_4$$

$$+ \frac{1}{45360} r^3 A_2^2 S^2 M^2 A_4 + \frac{-1}{60480} r^3 S A_2 M^4 A_4$$

$$+ \frac{1}{362880} r^3 M^6 A_4\right) \eta^9 + \left(\frac{1}{69300} r^3 S^3 A_4^2\right.$$

$$- \frac{13}{2494800} r^3 t^{11} S^3 A_4^2 A_2 + \frac{59}{9979200} r^3 M^2 S^2 A_4^2$$

$$- \frac{1}{1425600} r^3 A_4^2 S^2 A_2 M^2 + \frac{13}{19958400} r^3 S A_4^2 M^4$$

$$+ \frac{1}{831600} r^3 A_2^2 S^3 A_4^2\right) \eta^{11} + \left(\frac{-1}{8845200} r^3 S^3 A_4^3\right.$$

$$+ \frac{1}{13899600} r^3 S^3 A_4^3 A_2 + \frac{-1}{97297200} r^3 M^2 S^2 A_4^3\right)$$

$$\cdot \eta^{13} + \frac{83}{40864824000} r^3 S^3 A_4^4 \eta^{15},$$

$$\vdots$$

$$(49)$$

From Step 4 substituting (46)-(49) in (21), we get the analytical-approximate solution:

$$f(\eta) = A_2 \eta + \frac{1}{6} A_4 \eta^3 + \frac{1}{120} r \left(4 S A_4 + M^2 A_4\right) \eta^5$$

$$+ \left(\frac{1}{210} r^2 S^2 A_4 + \frac{1}{504} r^2 S M^2 A_4 - \frac{1}{630} r^2 A_2 S^2 A_4\right.$$

$$- \frac{1}{2520} r^2 S A_2 M^2 A_4 + \frac{1}{5040} r^2 M^4 A_4$$

$$+ \frac{1}{2520} r S A_4^2\right) \eta^7 + \left(\frac{-1}{45360} r^2 S^2 A_4^2 A_2\right.$$

$$+ \frac{1}{60480} r^2 M^2 S A_4^2 + \frac{1}{1890} r^3 S^3 A_4$$

$$+ \frac{13}{19958400} r^3 S A_4^2 A_2 + \frac{-1}{2268} r^3 A_2 S^3 A_4$$

$$+ \frac{-1}{5670} r^3 S^2 A_2 M^2 A_4 + \frac{1}{20160} r^3 S M^4 A_4$$

$$+ \frac{1}{11340} r^3 A_2^2 S^3 A_4 + \frac{1}{45360} r^3 A_2^2 S^2 M^2 A_4$$

$$+ \frac{-1}{60480} r^3 S A_2 M^4 A_4 + \frac{1}{362880} r^3 M^6 A_4\right) \eta^9 + . \tag{50}$$

5. Convergence Analysis

Here, we study the analysis of convergence for the analytical-approximate solution (50) resulting from the application of power series novel algorithm for solving the problem of the squeezing flow between two parallel plates.

Definition 1. Suppose that H is Banach space, R is the real number, and $G[F]$ is a nonlinear operator defined by $G[F]: H \longrightarrow R$. Then the sequence of the solutions generated by a new approach can be written as

$$F_{n+1} = G[F_n],$$

$$F_n = \sum_{k=0}^{n} f_k, \tag{51}$$

$$n = 0, 1, 2, 3, \ldots$$

where $G[F]$ satisfies Lipschitz condition such that, for $\alpha > 0$, $\alpha \in R$, we have

$$\|G[F_n] - G[F_{n-1}]\| \leqslant \alpha \|F_n - F_{n-1}\|. \tag{52}$$

Theorem 2. *The series of the analytical-approximate solution* $f(\eta) = \sum_{k=0}^{\infty} f_k(\eta)$ *generated by novel approach converge if the following condition is satisfied*

$$\|F_n - F_m\| \longrightarrow 0, \quad as \ m \longrightarrow \infty \tag{53}$$
$$for \ 0 \leqslant \alpha < 1.$$

Proof. From the above definition, we have

$$\|F_n - F_m\| = \left\| \sum_{k=0}^{n} f_k - \sum_{k=0}^{m} f_k \right\|,$$

$$= \left\| \left[f_0 + L^{-1} \sum_{k=1}^{n} \frac{d^{(k-1)} G[f_0(\eta)]}{d\eta^{(k-1)}} \right] \right.$$

$$\left. - \left[f_0 + L^{-1} \sum_{k=1}^{m} \frac{d^{(k-1)} G[f_0(\eta)]}{d\eta^{(k-1)}} \right] \right\|,$$

$$= \left\| L^{-1} G \left[\sum_{k=0}^{n-1} f_k \right] - L^{-1} G \left[\sum_{k=0}^{m-1} f_k \right] \right\|, \tag{54}$$

$$(since \ F_n = G[F_{n-1}])$$

$$\leqslant \left| Ł^{-1} \right| \left\| G \left[\sum_{k=0}^{n-1} f_k \right] - G \left[\sum_{k=0}^{m-1} f_k \right] \right\|,$$

$$\leqslant \left| L^{-1} \right| \left\| G[F_{n-1}] - G[F_{m-1}] \right\|,$$

$$\leqslant \alpha \left\| F_{n-1} - F_{m-1} \right\|,$$

since G[F] satisfies Lipschitz condition. Let $n = m + 1$; then

$$\|F_{m+1} - F_m\| \leqslant \alpha \|F_m - F_{m-1}\|, \tag{55}$$

and hence,

$$\|F_m - F_{m-1}\| \leqslant \alpha \|F_{m-1} - F_{m-2}\| \leqslant \cdots$$
$$\leqslant \alpha^{m-1} \|F_1 - F_0\|. \tag{56}$$

From (56) we get

$$\|F_2 - F_1\| \leqslant \alpha \|F_1 - F_0\|,$$
$$\|F_3 - F_2\| \leqslant \alpha^2 \|F_1 - F_0\|,$$
$$\|F_4 - F_3\| \leqslant \alpha^3 \|F_1 - F_0\|, \tag{57}$$
$$\vdots$$
$$\|F_m - F_{m-1}\| \leqslant \alpha^{m-1} \|F_1 - F_0\|.$$

Using triangle inequality

$$\|F_n - F_m\| = \|F_n - F_{n-1} - F_{n-2} - \cdots - F_{m+1} - F_m\|,$$

$$\leqslant \|F_n + F_{n-1}\| + \|F_{n-1} - F_{n-2}\| + \cdots + \|F_{m+1} - F_m\|,$$

$$\leqslant \left[\alpha^{n-1} + \alpha^{n-2} + \cdots + \alpha^m \right] \|F_1 - F_0\|, \tag{58}$$

$$= \alpha^m \left[\alpha^{n-m-1} + \alpha^{n-m-2} + \cdots + 1 \right] \|F_1 - F_0\|,$$

$$\leqslant \frac{\alpha^m}{1-\alpha} \|F_1 - F_0\|,$$

as $m \longrightarrow \infty$, we have $\|F_n - F_m\| \longrightarrow 0$, and then F_n is a Cauchy sequence in Banach space H. □

Theorem 3. *The solution* $f(\eta) = \sum_{k=0}^{\infty} f_k(\eta)$ *converges. This analytic solution will be close to the solution of problem (11)-(12) when the following property is achieved*

$$L^{-1} G[f] = \lim_{n \to \infty} L^{-1} [G[F_n]]. \tag{59}$$

Proof. For $F \in H$, define an operator for H to H by

$$J(F) = F_0 + L^{-1} G[F], \tag{60}$$

and let $F_1, F_2 \in H$; we have

$$\|J(F_1) - J(F_2)\|$$

$$= \left\| \left[F_0 + L^{-1} G[F_1] \right] - \left[F_0 + L^{-1} G[F_2] \right] \right\|,$$

$$= \left\| L^{-1} G[F_1] - L^{-1} G[F_2] \right\|, \tag{61}$$

$$\leqslant \left| L^{-1} \right| \left\| G[F_1] - G[F_2] \right\|,$$

$$\leqslant \gamma \|F_1 - F_2\|,$$

so, the mapping J is contraction, and by the Banach fixed-point theorem for contraction, there is a unique solution of problem (11)-(12). Now we prove that that the series solution $f(\eta)$ satisfies problem (11)-(12),

$$L^{-1} G[f] = L^{-1} G \left[\sum_{k=0}^{\infty} f_k \right],$$

$$= L^{-1} G \left[\lim_{n \to \infty} \sum_{k=0}^{n} f_k \right],$$

$$= L^{-1} G \left[\lim_{n \to \infty} F_n \right], \tag{62}$$

$$= \lim_{n \to \infty} L^{-1} G[F_n].$$

□

In practice, Theorems 2 and 3 suggest computing the value of α as described in the following definition.

Table 1: Comparison between analytical-approximate solution and numerical solution for $f(\eta)$ when $M = 0$ and $\gamma \longrightarrow \infty$.

S	Wang [7]	Present results
0.97800	-2.19100	-2.19900
0.00000	-3.00000	-3.00000
-0.49770-	-2.61930	-2.61910
-0.09998	-2.92770	-2.92770
0.09403	-3.06630	-3.06630
0.43410	-3.29400	-3.29400
0.12240	-3.70800	-3.70500

Definition 4. For $k = 1, 2, 3, \ldots$

$$\alpha^k = \begin{cases} \dfrac{\|F_{k+1} - F_k\|}{\|F_1 - F_0\|} = \dfrac{\|f_{k+1}\|}{\|f_1\|}, & \|f_1\| \neq 0, \\ 0, & \|f_1\| = 0, \end{cases} \tag{63}$$

and, now, we will apply Definition 4 on the squeezing flow between two parallel plates to find convergence; then we obtain, for example, the following:

if we put $S = -1$, $M = 1$, $A_2 = 1.511619152$, $A_4 = -3.143837395$, $\gamma = 0.2$, the value of α will be

$$\begin{aligned} & \|F_2 - F_1\|_2 \leqslant \alpha \|F_1 - F_0\|_2 \implies \\ & \quad \alpha = 0.0078755538 < 1, \\ & \|F_3 - F_2\|_2 \leqslant \alpha^2 \|F_1 - F_0\|_2 \implies \\ & \quad \alpha^2 = 0.0000248127 < 1, \\ & \|F_4 - F_3\|_2 \leqslant \alpha^3 \|F_1 - F_0\|_2 \implies \\ & \quad \alpha^3 = 0.00000019828 < 1, \\ & \qquad \qquad \vdots \\ & \|F_2 - F_1\|_{+\infty} \leqslant \alpha \|F_1 - F_0\|_{+\infty} \implies \\ & \quad \alpha = 0.0078442924 < 1, \\ & \|F_3 - F_2\|_{+\infty} \leqslant \alpha^2 \|F_1 - F_0\|_{+\infty} \implies \\ & \quad \alpha^2 = 0.000017816 < 1, \\ & \|F_4 - F_3\|_{+\infty} \leqslant \alpha^3 \|F_1 - F_0\|_{+\infty} \implies \\ & \quad \alpha^3 = 0.0000001976 < 1, \\ & \qquad \qquad \vdots \end{aligned} \tag{64}$$

Also, if we choose $S = 1$, $M = 1$, $\gamma = 0.2$, $A_2 = 1.481186659$, $A_4 = -2.772867578$, then we obtain

$$\begin{aligned} & \|F_2 - F_1\|_2 \leqslant \alpha \|F_1 - F_0\|_2 \implies \\ & \quad \alpha = 0.016036663 < 1, \\ & \|F_3 - F_2\|_2 \leqslant \alpha^2 \|F_1 - F_0\|_2 \implies \\ & \quad \alpha^2 = 0.0001172840 < 1, \\ & \|F_4 - F_3\|_2 \leqslant \alpha^3 \|F_1 - F_0\|_2 \implies \\ & \quad \alpha^3 = 0.0000007283831966 < 1, \\ & \qquad \qquad \vdots \\ & \|F_2 - F_1\|_{+\infty} \leqslant \alpha \|F_1 - F_0\|_{+\infty} \implies \\ & \quad \alpha = 0.0160223281 < 1, \\ & \|F_3 - F_2\|_{+\infty} \leqslant \alpha^2 \|F_1 - F_0\|_{+\infty} \implies \\ & \quad \alpha^2 = 0.0001140572 < 1, \\ & \|F_4 - F_3\|_{+\infty} \leqslant \alpha^3 \|F_1 - F_0\|_{+\infty} \implies \\ & \quad \alpha^3 = 0.0000006301 < 1, \\ & \qquad \qquad \vdots \end{aligned} \tag{65}$$

Then $\sum_{k=0}^{\infty} f_k(\eta)$ converges to the solution $f(\eta)$ when $0 \leqslant \alpha^k < 1$, $k = 1, 2, \ldots$.

6. Results and Discussions

In this section the influences of the squeeze number S, Casson fluid parameter γ, and the magnetic number M on the axial $f(\eta)$ and radial $f'(\eta)$ velocities have been represented. Table 1 shows a comparison between the present results obtained from a novel algorithm and the numerical results introduced by Wang [7], while Table 2 shows a comparison between the collected results with variation of parameter method (VPM) [21]. It was noted that the solution of the present algorithm is in agreement with these methods. The convergence of the of values $f'(0)$ and $f'''(0)$ is indicated in Table 3. Table 4 illustrates the numerical values of skin friction coefficient which can be observed from an increase of all the parameters leading to an increase of a magnitude of the skin friction coefficient. Subsequently, there is also a comparison with variation parameter method (VPM) so that the results appear relatively convergent. A comparison between the analytical-approximate solution and the numerical solution for the axial and radial velocities was shown in Tables 5 and 6. These tables clearly demonstrated that the solution has approximate manner. In Figures 2–7 there are two cases with regard to the squeeze number S; three figures show the case when the plates are moving apart $S > 0$. In the other case there are three

TABLE 2: Comparison of $f(\eta)$ for $M = 1$ and $\gamma = 0.4$.

η	$S = 5$			$S = -5$		
	Present results	VPM [21]	$RK - 4$	Present results	VPM [21]	$RK - 4$
0.1	0.139103	0.139081	0.139104	0.166665	0.166839	0.166663
0.2	0.276402	0.276358	0.276405	0.328112	0.328444	0.328107
0.3	0.409981	0.409918	0.409984	0.479402	0.479861	0.479396
0.4	0.537705	0.537628	0.537709	0.616144	0.616685	0.616137
0.5	0.657098	0.537628	0.657105	0.734719	0.735286	0.734713
0.6	0.765208	0.765125	0.765217	0.832465	0.832992	0.832461
0.7	0.858455	0.858383	0.858467	0.907792	0.908218	0.907797
0.8	0.932458	0.932408	0.932471	0.960237	0.960506	0.960270
0.9	0.981839	0.981819	0.981843	0.990434	0.990529	0.990550

TABLE 3: Convergence of analytical-approximate solution for $M = 1$ and $\gamma = 0.2$.

order of approximations	$S = 1$		$S = -1$	
	A_2	A_4	A_2	A_4
2 terms	1.481730942	-2.777709528	1.511797484	-3.145960580
3 terms	1.481190867	-2.772901421	1.511619398	-3.143838923
4 terms	1.481186624	-2.772867340	1.511619138	-3.143837287
5 terms	1.481186658	-2.772867569	1.511619153	-3.143837398
6 terms	1.481186659	-2.772867578	1.511619152	-3.143837395
7 terms	1.481186659	-2.772867578	1.511619152	-3.143837395
8 terms	1.481186659	-2.772867578	1.511619152	-3.143837395

TABLE 4: Comparison of the values for skin friction coefficient $(1 + 1/\gamma)f''(1)$.

S	γ	M	present results	VPM [19]
-5	0.4	1	-6.3949610	-6.2987080
-3	0.4	1	-8.3207270	-8.3207270
-1	0.4	1	-9.9705750	-9.9703760
1	0.4	1	-11.375837	-11.376240
3	0.4	1	-12.604612	-12.610669
5	0.4	1	-13.697927	-13.718095
-3	0.1	1	-30.991843	-30.991005
-3	0.3	1	-10.851771	-10.873387
-3	0.5	1	-6.7896240	-6.7715490
3	0.1	1	-35.260196	-35.260196
3	0.3	1	-15.145259	-15.149577
3	0.5	1	-11.071084	-11.078736
-3	0.4	2	-9.0435300	-9.0381960
-3	0.4	4	-11.532951	-11.531981
-3	0.4	6	-14.819321	-14.819321
3	0.4	2	-13.092241	-13.101572
3	0.4	4	-14.908219	-14.908219
3	0.4	6	-17.471534	-17.501183

figures when dilating plates $S < 0$. These cases explain the effects of physical parameters and studying the path of the curves $f(\eta)$ and $f'(\eta)$ between parallel plates. The results of these cases can be summarized in the following points:

(i) *The first case $S > 0$*: Figure 2 shows the effects of increasing values of squeeze number S on the axial velocity and average of radial velocity. This Figure also indicates that an increase of S leads to a decrease of $f(\eta)$. In addition, the curves of $f(\eta)$ are started from the top plate towards the bottom plate according to the increase in S for $0 < \eta < 1$, while for $f'(\eta)$ the same case occurred until $\eta \leq 0.5$, and the reverse situation of its curves happened for $0.5 < \eta \leq 1$. The magnetic number M and Casson fluid parameter γ on $f(\eta)$ and $f'(\eta)$ were described in Figures 3 and 4 respectively. It can be observed that increasing M and γ leads to decrease of $f(\eta)$ for the positive value of squeeze number S. Moreover the increase of M and γ on $f'(\eta)$ for the positive value of squeeze number S proves the similar behavior in case of the increase in S.

(ii) *The second case $S < 0$*: Figure 5 illustrates the effects of the negative values for the squeezing number S showing that the decrease of S values causes increasing in axial velocity. This figure demonstrates that the curves of $f(\eta)$ which starts from the bottom plate towards the top plate tend to decrease S for $0 < \eta < 1$, while for $f'(\eta)$, it was found that the same case happened when $\eta \leq 0.4$, and the reverse situation of their curves happened for $0.4 < \eta \leq 1$. Figure 6 indicates an effect of magnetic number M for axial and radial velocity. This effect is similar to the effect of M in the positive value of squeeze number S

Table 5: Comparison between the solution of present algorithm and $RK-4$ algorithm for $M=1$, $\gamma = 0.2$, $S = 1$.

| η | $f(\eta)$ | | $f'(\eta)$ | |
	Present results	$RK-4$	Present results	$RK-4$
0.1	0.147656	0.147656	1.467313	1.467313
0.2	0.292534	0.292534	1.425575	1.425575
0.3	0.431831	0.431832	1.355629	1.355629
0.4	0.562701	0.562701	1.256898	1.256899
0.5	0.682225	0.682226	1.128583	1.128583
0.6	0.787397	0.787398	0.969661	0.969661
0.7	0.875096	0.875097	0.778889	0.778881
0.8	0.942065	0.942067	0.554821	0.554821
0.9	0.984895	0.984897	0.295804	0.295804

Table 6: Comparison between the solution of present algorithm and $RK-4$ algorithm for $M=1$, $\gamma = 0.2$, $S = -1$.

| η | $f(\eta)$ | | $f'(\eta)$ | |
	Present results	$RK-4$	Present results	$RK-4$
0.1	0.150638	0.150638	1.485907	1.495907
0.2	0.298136	0.298136	1.448847	1.448847
0.3	0.439360	0.439361	1.370673	1.370673
0.4	0.571246	0.571246	1.261767	1.261767
0.5	0.690716	0.690716	1.122650	1.122650
0.6	0.794791	0.794790	0.953971	0.953971
0.7	0.880550	0.880541	0.756487	0.756487
0.8	0.945156	0.945156	0.531047	0.531047
0.9	0.985858	0.985876	0.278565	0.278566

on $f(\eta)$ and $f'(\eta)$ but the point of intersection of the curves $f'(\eta)$ is $\eta = 0.4$. Figure 7 demonstrates the effects of Casson fluid parameter γ for axial and radial velocity; it was also noted from this figure that the increasing of γ causes increasing of $f(\eta)$. Subsequently, the movement of the curves of $f(\eta)$ occurs from the bottom plate across the top plate due to an increase of γ for $0 < \eta < 1$, whereas the same situation of $f'(\eta)$ occurs when $\eta \le 0.4$, and the reverse case of their curves occurs when $0.4 < \eta \le 1$.

From the above two cases, it can be seen that the curves of $f(\eta)$ and $f'(\eta)$ are different in distance between them, where in $S > 0$ it is wide; then $S < 0$. However they have the same behavior. Moreover, the bifurcation of $f'(\eta)$ in $S > 0$ happened when $\eta = 0.5$ and for $S < 0$ happened when $\eta = 0.4$. Generally, it seems that the curve of $f(\eta)$ is increasing with increasing of η for all values of S, M, and γ while the curve of $f'(\eta)$ is decreasing with increasing of η for all above values. As for the effects of different physical parameters (the squeezing number S, Casson fluid parameter γ, the magnetic number M) and the values α, l on the velocity components $u(x, y, t)$, $v(x, y, t)$ and the vorticity $\omega(x, y, t)$, the following can be concluded:

(i) In the case that the physical parameters and the values α, l are constants (when there is a change in the squeezing number), the surfaces are almost identical except for the surface $v(x, y, t)$. This case shows a slight change which is a little curvature as indicated in Figures 8 and 9. However, there is a change in the surfaces, when $\alpha < 0$ and $S \ge 11$ with a change in the surface of $w(x, y, t)$, while the surfaces of $u(x, y, t)$ and $v(x, y, t)$ remain similar.

(ii) There is no change of other fixations values on the surfaces when a change happened in the parameter M or γ as shown in Figures 10–14. But there is change in the surfaces $u(x, y, t)$, $w(x, y, t)$, and $v(x, y, t)$ when $\alpha < 0$, $S \le -14$, $M \le 4$, and $\gamma \ge 0.4$ with observing that the surface $v(x, y, t)$ simply changes when $M = 4$ in Figure 11 and $\gamma = 0.4$ in Figure 14.

(iii) All the physical parameters are constants except a change in their values α even if they are positive or negative. Each value of α shows that the surface is different from the other values of $u(x, y, t)$, $v(x, y, t)$, and $\omega(x, y, t)$. It was also noticed that the surface $v(x, y, t)$ takes the negative values of α inversely with the surface $v(x, y, t)$ that has a positive value of α. This can be seen in Figures 15 and 16.

(iv) Finally, Figures 17–19 show that there is no change in other fixations values on the surfaces $u(x, y, t)$, $\omega(x, y, t)$, and $v(x, y, t)$ when a change happened in value l. But there is change in the surfaces when $\alpha < 0$, $-1.5 < l < 1.5$ for $u(x, y, t)$, $\omega(x, y, t)$,
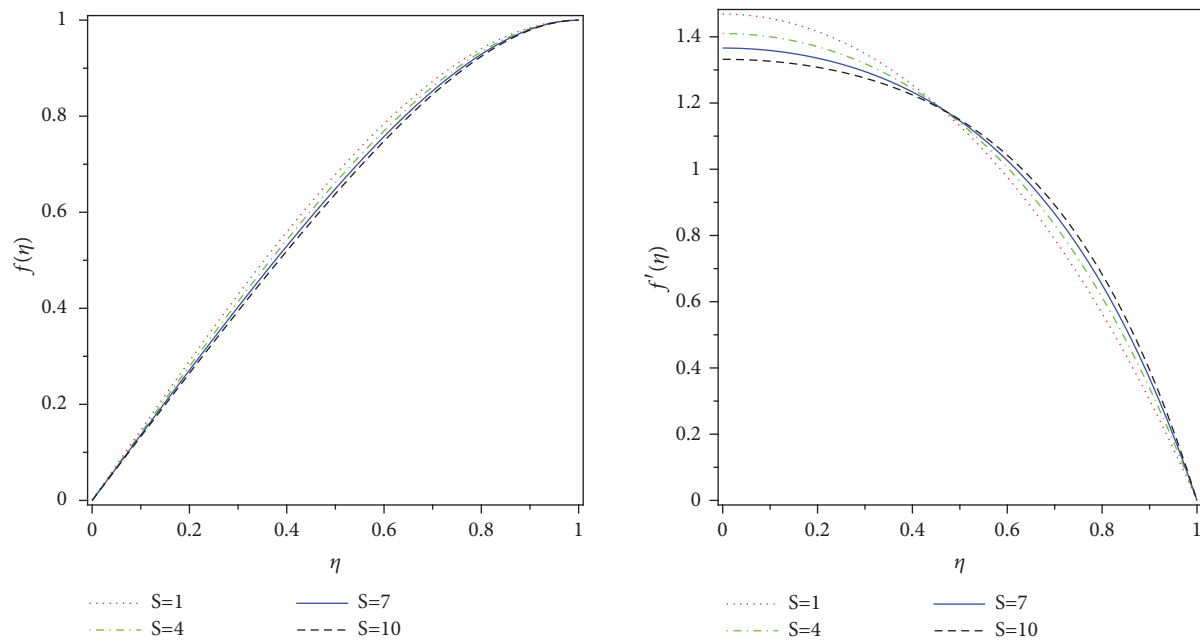
FIGURE 2: $f(\eta)$ and $f'(\eta)$ for positive values S when $M = 1$, $\gamma = 0.4$.
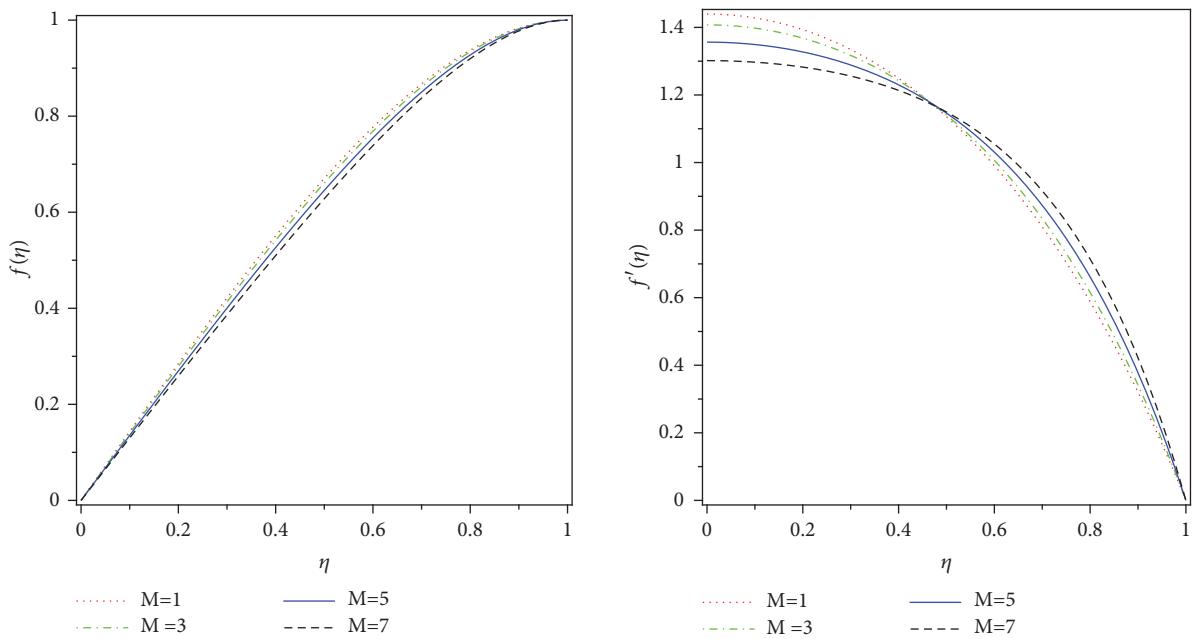
FIGURE 3: $f(\eta)$ and $f'(\eta)$ for the values M when $S = 3$, $\gamma = 0.3$.

and $v(x, y, t)$ with noticing that the surface $v(x, y, t)$ slightly changes when $l = 1$ in Figure 18.

Physically, magneto field parameter M is increased; this leads to stronger Lorentz force along the vertical direction which offers more resistance to the flow. The velocity profiles exponentially decay to zero at shorter distances when either M or γ is increased. This indicates that increase in either M or γ leads to thinner boundary layer. Casson fluid

between parallel plates is a non-Newtonian fluid and its parameter γ corresponds to viscosity in Newtonian fluid. Thus the increasing of γ leads to increase of viscous force and decrease of the velocity of fluid. The squeezing number S includes the flow which results from a movement of the two parallel plates with a fluid apart. The geometric explanation can be summarized as the magnetic field is applied to electrical conducting fluid which accompanies an increase of S leading to increase of the velocity of the
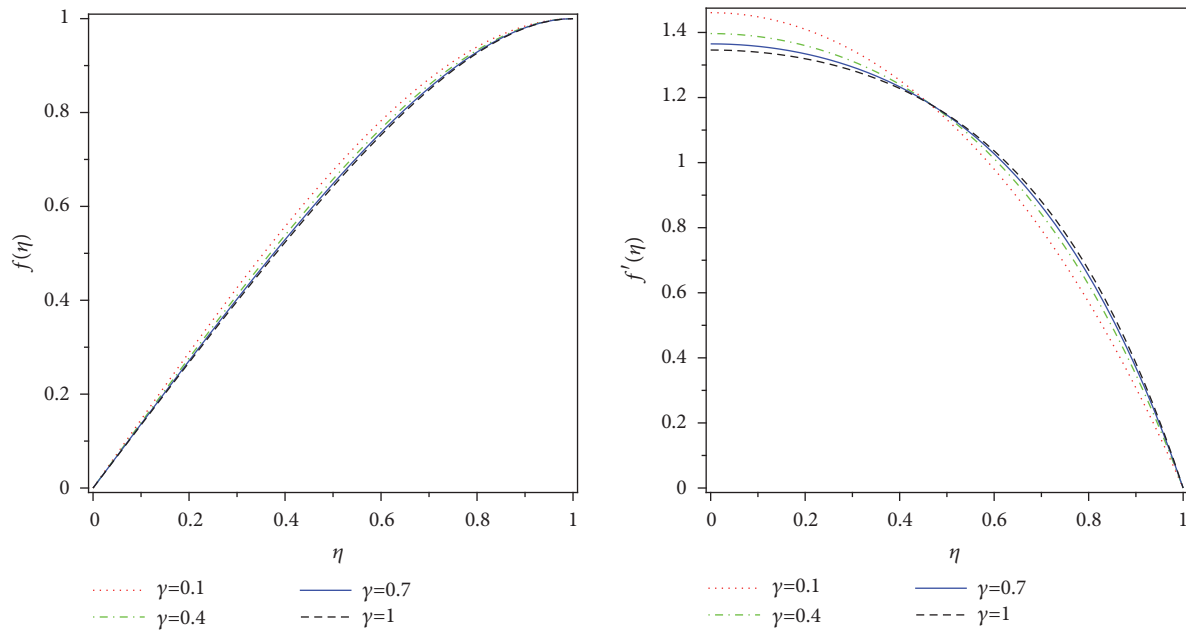
FIGURE 4: $f(\eta)$ and $f'(\eta)$ for the values γ when $M = 2$, $S = 4$.
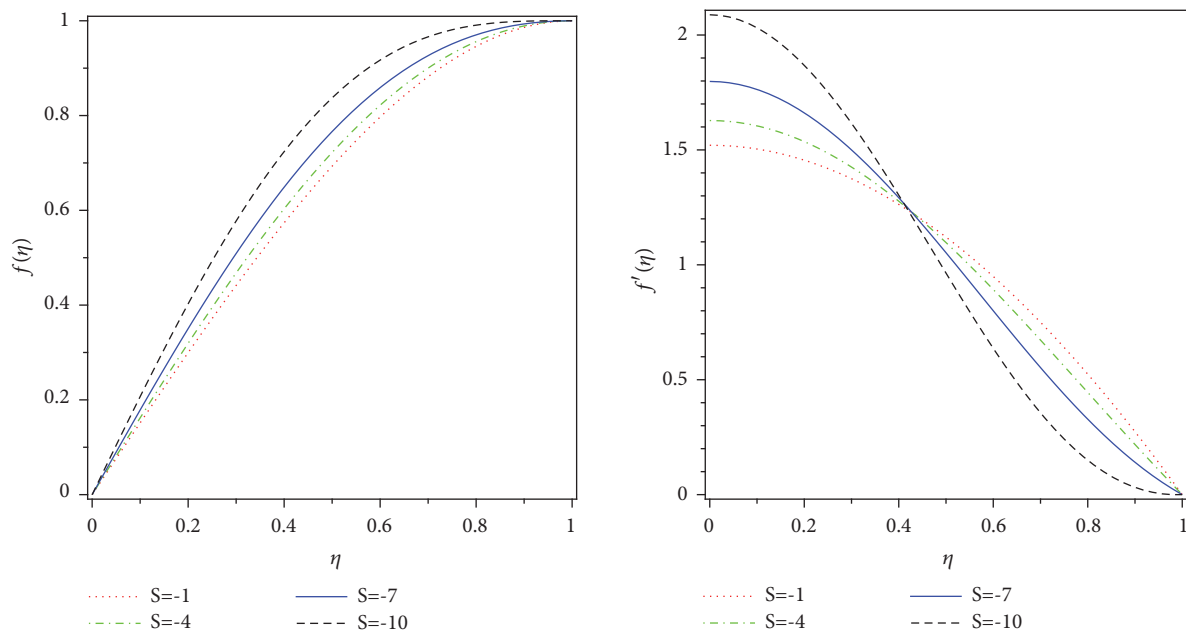
FIGURE 5: $f(\eta)$ and $f'(\eta)$ for negative values S when $M = 1$, $\gamma = 0.4$.

fluid. This helps to generate a magnetic normal force to the direction of the magnetic field. Current geometry in this case comprises the magnetic field which is applied in a perpendicular direction to generate a force in x-direction. This force can reduce the movement of the fluid; therefore, the magnetic field is used to control or reduce the movement of the fluid.

7. Conclusions

In this paper, a novel algorithm for analytic technique based on the coefficients of power series resulting from integrating nonlinear differential equations with appropriate conditions is proposed, and it is employed to obtain a new analytical-approximate solution for unsteady
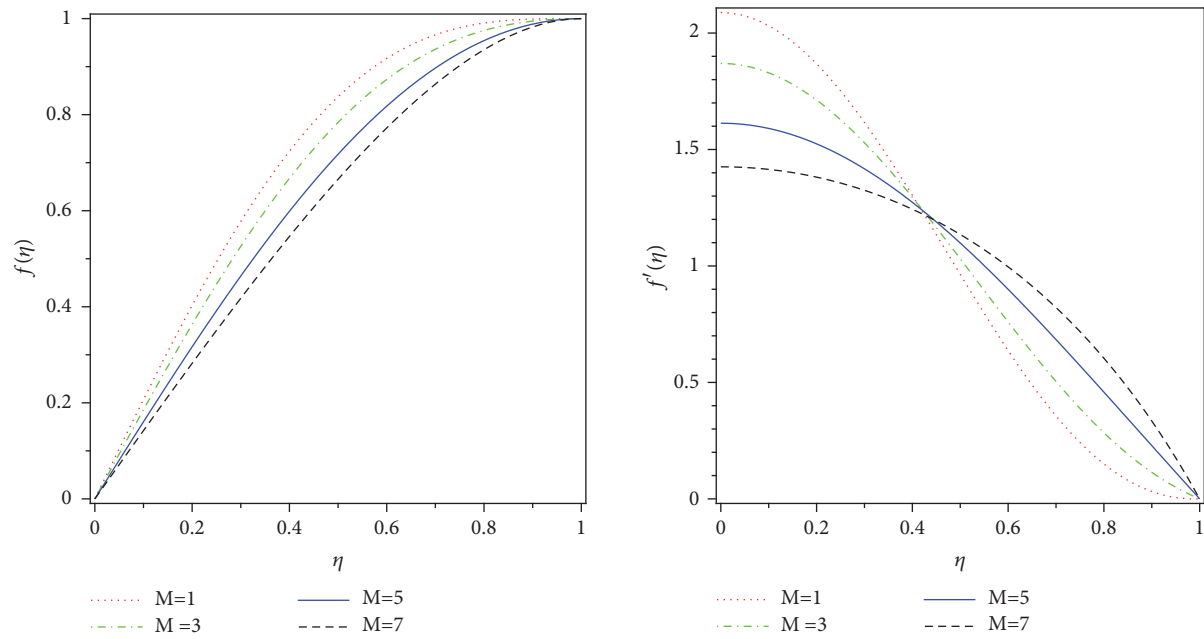
FIGURE 6: $f(\eta)$ and $f'(\eta)$ for the values M when $S = -10$, $\gamma = 0.4$.
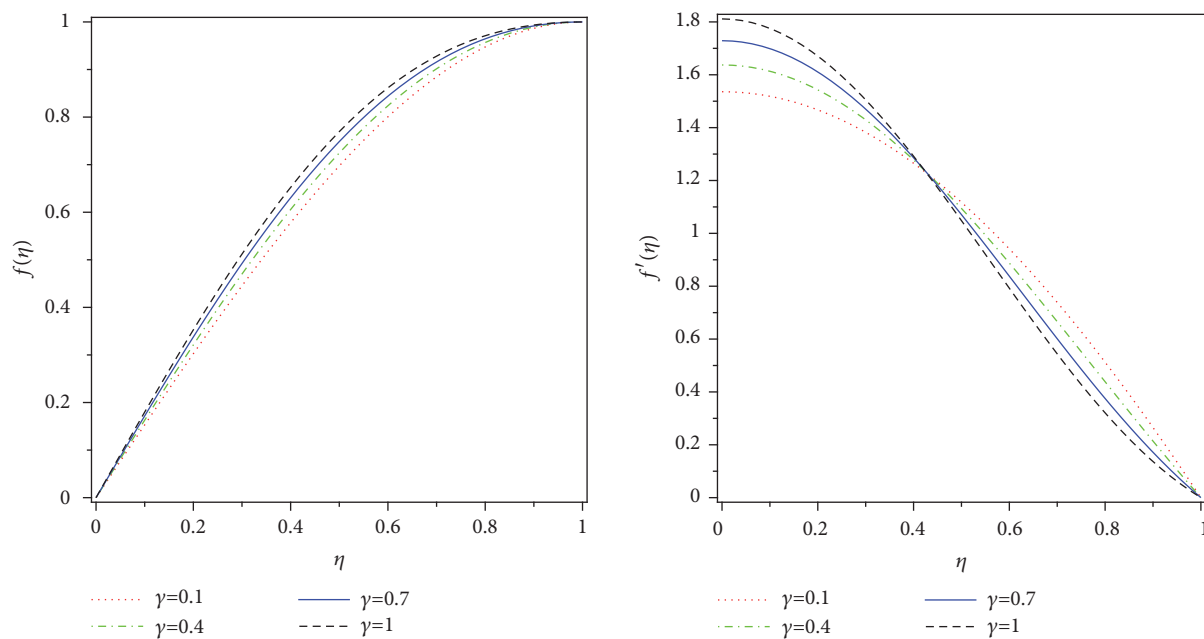
FIGURE 7: $f(\eta)$ and $f'(\eta)$ for the values γ when $M = 2$, $S = -5$.

two-dimensional nonlinear squeezing flow between two parallel plates successfully. It has been found that the construction of the novel algorithm possessed good convergent series and the convergence of the results is shown explicitly. Graphs and tables are presented to investigate the influence of physical parameters on the velocity. Convergence analysis is carried out to back up the validity of the novel algorithm and check its computational efficiency. Analysis of the converge

confirms that the novel algorithm is an efficient technique as compared to other methods presented in this work. As can be seen from the comparison, the computational results of the present solution and the results of other solutions are identical with 5 or 6 decimal places. It is noted that a magnetic field is a control phenomenon in many flows and it could be employed to normalize the flow behavior. Moreover, a squeeze number plays an important role in these
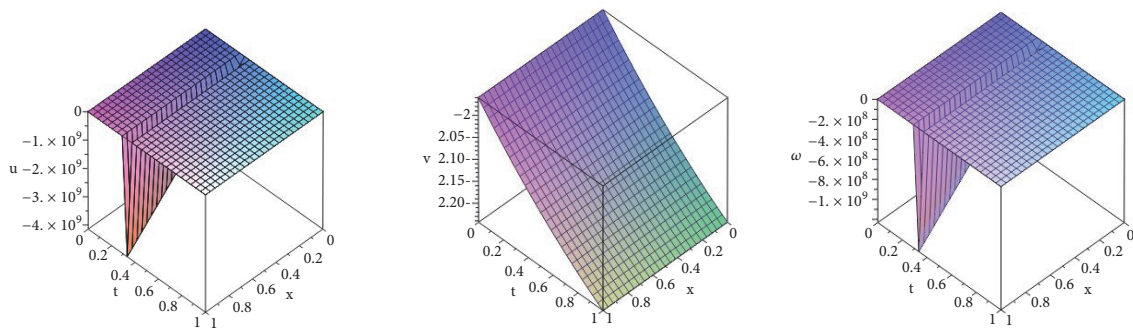
FIGURE 8: Surface of u, v, and ω for $M = 1$, $\mathbf{S = 5}$, $\gamma = 0.5$, $y = 1$, $\alpha = 3$, $l = 2$.
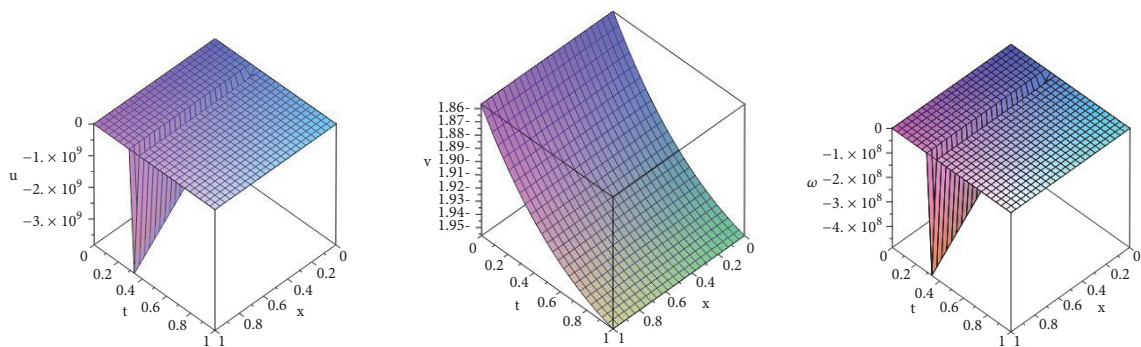
FIGURE 9: Surface of u, v, and ω for $M = 1$, $\mathbf{S = 15}$, $\gamma = 0.5$, $y = 1$, $\alpha = 3$, $l = 2$.
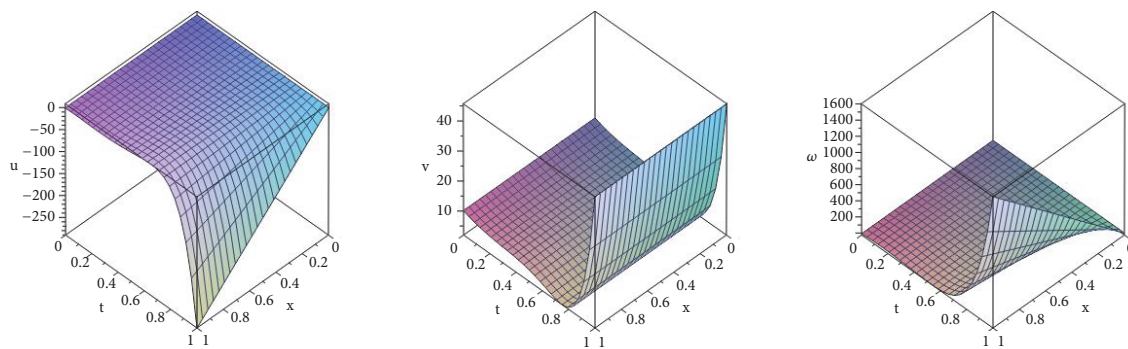
FIGURE 10: Surface of u, v, and ω for $\mathbf{M = 1}$, $S = -15$, $\gamma = 0.5$, $y = 1$, $\alpha = -4$, $l = 2$.
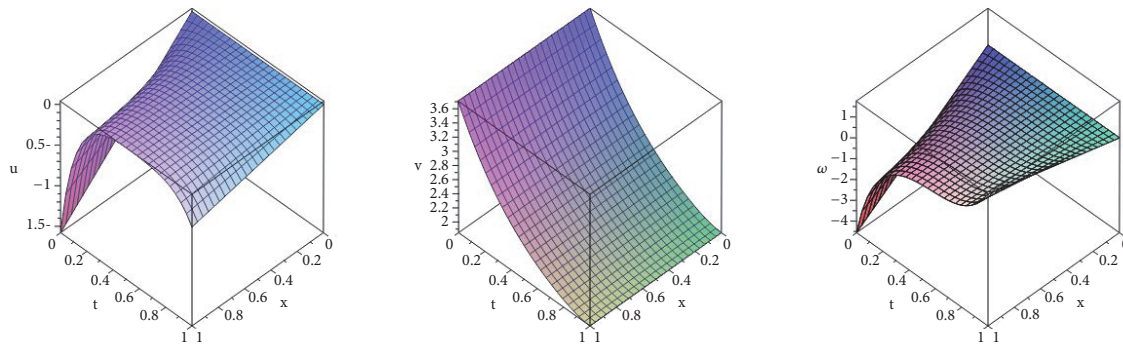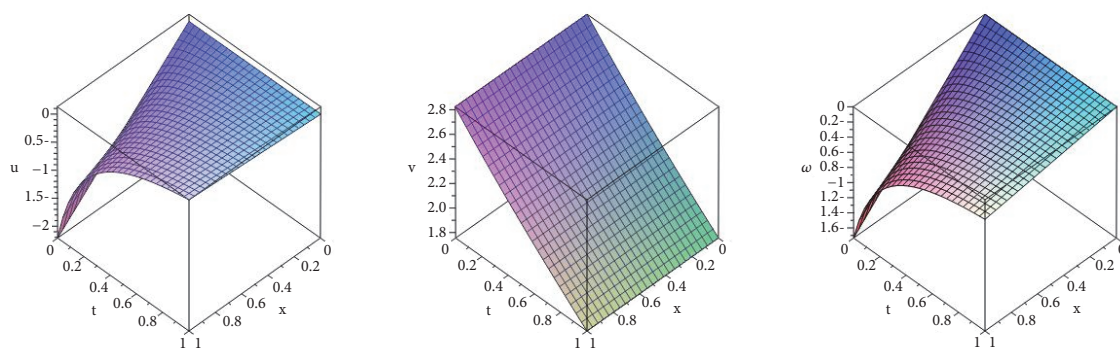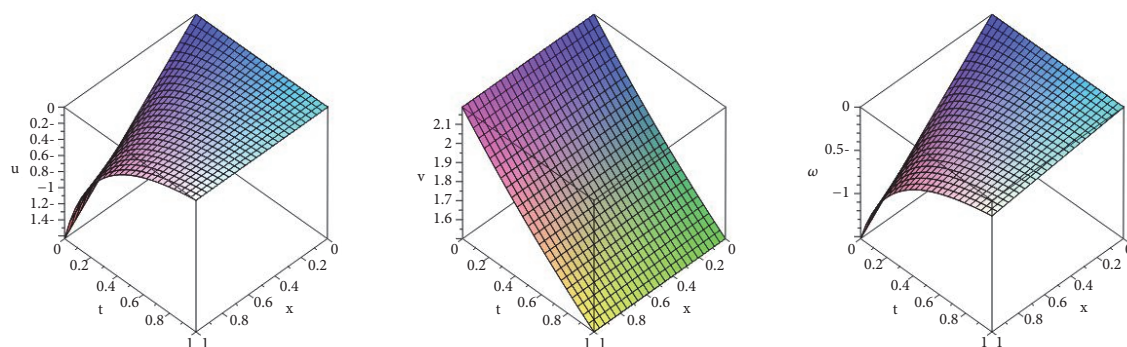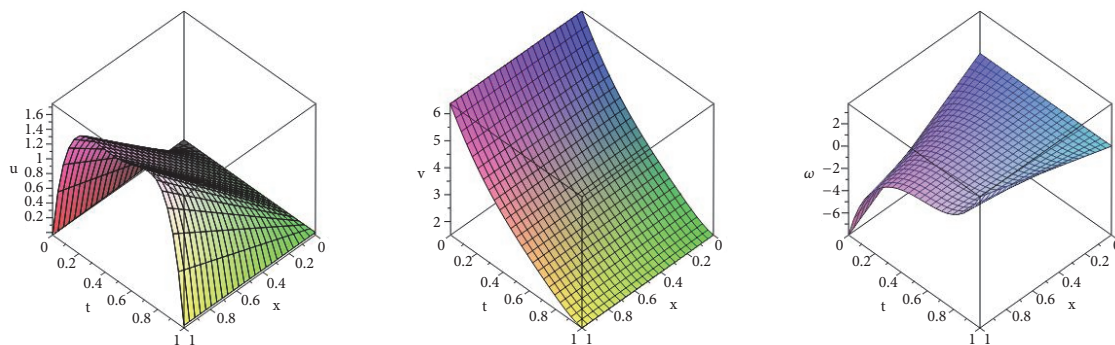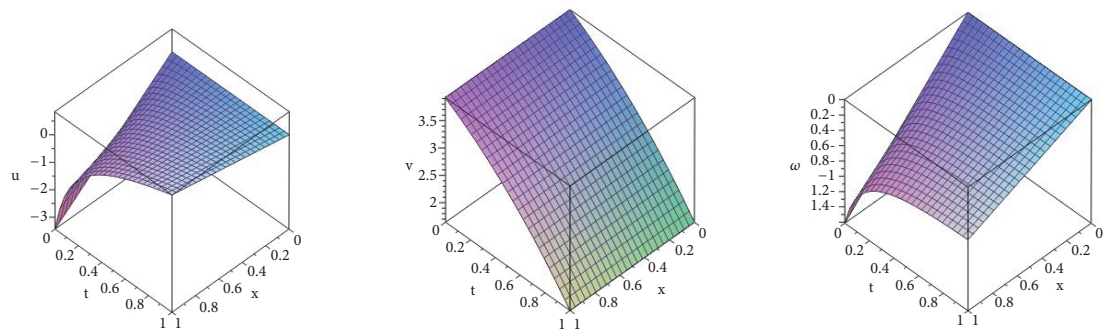

FIGURE 11: Surface of u, v, and ω for $\mathbf{M = 4}$, $S = -15$, $\gamma = 0.5$, $y = 1$, $\alpha = -4$, $l = 2$.

FIGURE 12: Surface of u, v, and ω for $\mathbf{M} = \mathbf{7}$, $S = -15$, $\gamma = 0.5$, $y = 1$, $\alpha = -4$, $l = 2$.

FIGURE 13: Surface of u, v, and ω for $M = 1$, $S = -14$, $\gamma = \mathbf{0.1}$, $y = 1$, $\alpha = -3$, $l = 2$.

FIGURE 14: Surface of u, v, and ω for $M = 1$, $S = -14$, $\gamma = \mathbf{0.4}$, $y = 1$, $\alpha = -3$, $l = 2$.

FIGURE 15: Surface of u, v, and ω for $M = 1$, $S = 5$, $\gamma = 0.5$, $y = 1$, $\alpha = \mathbf{-6}$, $l = 2$.
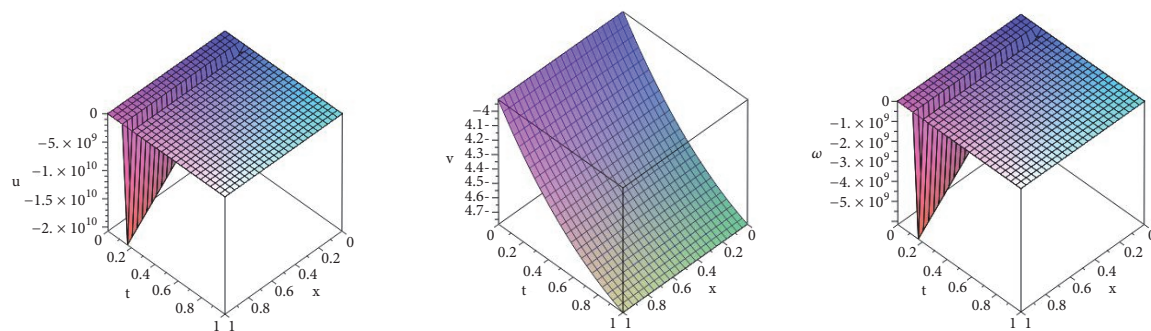
FIGURE 16: Surface of u, v, and ω for $M = 1$, $S = 5$, $\gamma = 0.5$, $y = 1$, $\alpha = \mathbf{6}$, $l = 2$.
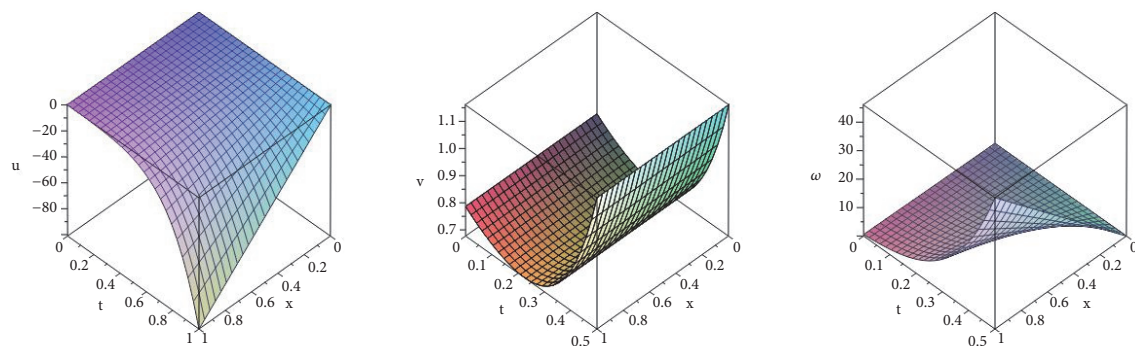

FIGURE 17: Surface of u, v, and ω for $M = 2$, $S = -10$, $\gamma = 0.3$, $y = 1$, $\alpha = -2$, $\mathbf{l = 0.8}$.
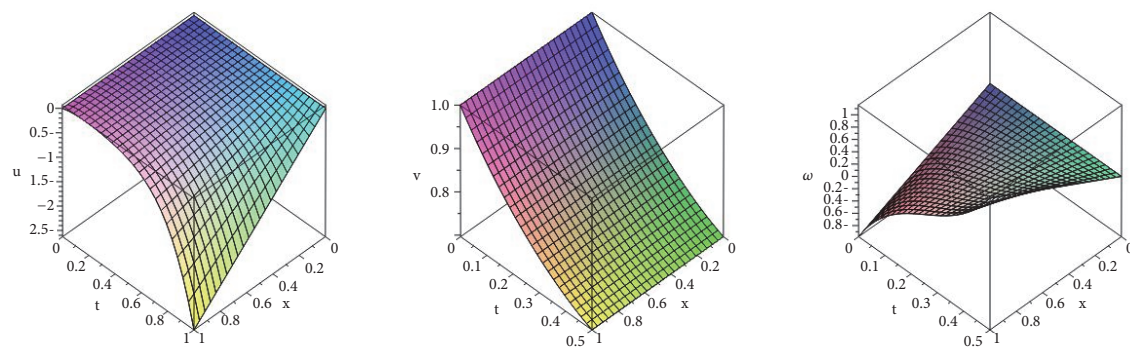

FIGURE 18: Surface of u, v, and ω for $M = 2$, $S = -10$, $\gamma = 0.3$, $y = 1$, $\alpha = -2$, $\mathbf{l = 1}$.
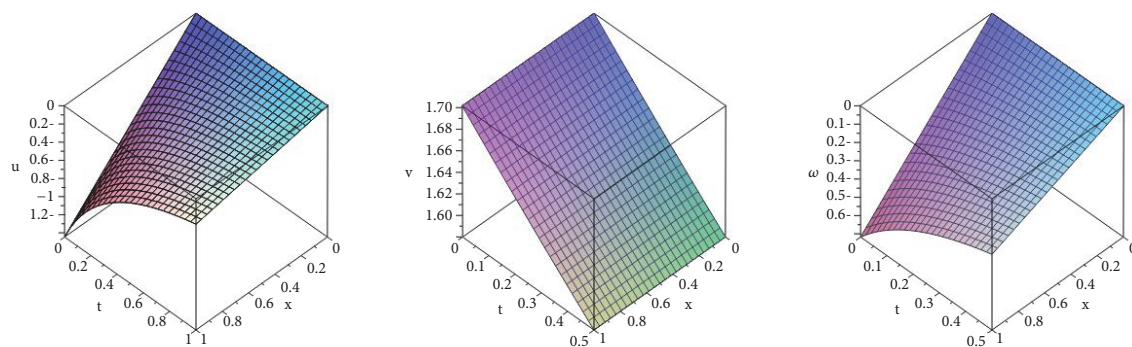

FIGURE 19: Surface of u, v, and ω for $M = 2$, $S = -10$, $\gamma = 0.3$, $y = 1$, $\alpha = -2$, $\mathbf{l = 3}$.

types of problems as increasing the squeeze number leads to increase in the velocity profile. The graphs which have a strong magnetic field were used to enhance the flow when the plates came together. In addition, the squeeze number increased the velocity profile when the plates become closer and going apart.

Data Availability

The data used to support the findings of this study are available from the corresponding author upon request.

Conflicts of Interest

The authors declare that they have no conflicts of interest.

Acknowledgments

References

[1] M. J. Stefan, "Versuch Uber die scheinbare adhesion," *Akad Wissensch Wien Math Natur*, vol. 69, p. 713, 1874.

[2] O. Reynolds, "On the theory of lubrication and its application to Mr. Beauchamp tower's experiments including an experimental determination of the viscosity of olive oil," *Philosophical Transactions of the Royal Society A*, vol. 177, pp. 157–234, 1886.

[3] F. R. Archibald, "Load capacity and time relations for squeeze films," *Journal of Lubrication Technology*, vol. 78, pp. A231–A245, 1956.

[4] J. D. Jackson, "A study of squeezing flow," *Applied Scientific Research*, vol. 11, no. 1, pp. 148–152, 1963.

[5] R. Usha and R. Sridharan, "Arbitrary squeezing of a viscous fluid between elliptic plates," *Fluid Dynamics Research*, vol. 18, no. 1, pp. 35–51, 1996.

[6] R. I. Yahaya, N. M. Arifin, and S. S. P. M. Isa, "Stability analysis on magnetohydrodynamic flow of casson fluid over a shrinking sheet with homogeneous-heterogeneous reactions," *Entropy*, vol. 20, no. 9, 2018.

[7] C. Y. Wang, "The squeezing of a fluid between two plates," *Journal of Applied Mechanics*, pp. 579–583, 1979.

[8] Y. Bouremel, "Explicit series solution for the Glauert-jet problem by means of the homotopy analysis method," *Communications in Nonlinear Science and Numerical Simulation*, vol. 12, no. 5, pp. 714–724, 2007.

[9] M. M. Rashidi, H. Shahmohamadi, and S. Dinarvand, "Analytic approximate solutions for unsteady two-dimensional and axisymmetric squeezing flows between parallel plates," *Mathematical Problems in Engineering*, vol. 2008, Article ID 935095, 13 pages, 2008.

[10] G. Domairry and A. Aziz, "Approximate analysis of MHD squeeze flow between two parallel disk with sunction or injection by homotopy perturbuation method," *Mathematical Problems in Engineering*, vol. 2009, Article ID 603916, 19 pages, 2009.

[11] X. J. Ran, Q. Y. Zhu, and Y. Li, "An explicit series solution of the squeezing flow between two infinite plates by means of the homotopy analysis method," *Communications in Nonlinear Science and Numerical Simulation*, vol. 14, no. 1, pp. 119–132, 2009.

[12] Z. Makukula, S. Motsa, and P. Sibanda, "On a new solution for the viscoelastic squeezing flow between two parallel plates," *Journal of Advanced Research in Applied Mathematics*, vol. 2, no. 4, pp. 31–38, 2010.

[13] M. Sheikholeslami, D. D. Ganji, and H. R. Ashorynejad, "Investigation of squeezing unsteady nanofluid flow using ADM," *Powder Technology*, vol. 239, pp. 259–265, 2013.

[14] U. Khan, S. I. Khan, N. Ahmed, S. Bano, and S. T. Mohyud-Din, "Heat transfer analysis for squeezing flow of a Casson fluid between parallel plates," *Ain Shams Engineering Journal*, vol. 7, no. 1, pp. 497–504, 2016.

[15] H. M. Duwairi, B. Tashtoush, and R. A. Damseh, "On heat transfer effects of a viscous fluid squeezed and extruded between two parallel plates," *Heat and Mass Transfer*, vol. 41, no. 2, pp. 112–117, 2004.

[16] S. T. Mohyud-Din, Z. A. Zaidi, U. Khan, and N. Ahmed, "On heat and mass transfer analysis for the flow of a nanofluid between ratating parallel plates," *Aerospace Science and Technology*, vol. 46, Article ID 4692014, pp. 514–522, 2014.

[17] S. T. Mohyud-Din and S. I. Khan, "Nonlinear radiation effects on squeezing flow of a Casson fluid between parallel disks," *Aerospace Science and Technology*, vol. 48, pp. 186–192, 2016.

[18] N. Ahmed, U. Khan, X. J. Yang, Z. A. Zaidi, and S. T. Mohyud-Din, "Magneto hydrodynamic (MHD) squeezing flow of a Casson fluid between parallel disks," *International Journal of Physical Sciences*, vol. 8, pp. 1788–1799, 2013.

[19] U. Khan, N. Ahmed, Z. A. Zaidi, M. Asadullah, and S. T. Mohyud-Din, "MHD squeezing flow between two infinite plates," *Ain Shams Engineering Journal*, vol. 5, no. 1, pp. 187–192, 2014.

[20] T. Hayat, A. Yousaf, M. Mustafa, and S. Obaidat, "(MHD) squeezing flow of second-grade fluid between two parallel disks," *International Journal for Numerical Methods in Fluids*, vol. 69, no. 2, pp. 399–410, 2012.

[21] N. Ahmed, U. Khan, S. I. Khan, S. Bano, and S. T. Mohyud-Din, "Effects on magnetic field in squeezing flow of a Casson fluid between parallel plates," *Journal of King Saud University - Science*, vol. 29, no. 1, pp. 119–125, 2017.

[22] S. Nadeem, R. Mehmood, and N. S. Akbar, "Optimized analytical solution for oblique flow of a Casson-nano fluid with convective boundary conditions," *International Journal of Thermal Sciences*, vol. 78, pp. 90–100, 2014.